AD-A216 976

ASSIFIED
CLASSIFICATION OF THIS PAGE

MASTER COPY

FOR REPRODUCTION PURPOSES

2

REPORT DOCUMENTATION PAGE

1a. SECURITY CLASSIFICATION Unclassified	1b. RESTRICTIVE MARKINGS
2a. SECURITY CLASSIFICATION AUTHORITY	3. DISTRIBUTION/AVAILABILITY OF REPORT Approved for public release; distribution unlimited.
2b. DECLASSIFICATION/DOWNGRADING SCHEDULE	
4. PERFORMING ORGANIZATION REPORT NUMBER(S)	5. MONITORING ORGANIZATION REPORT NUMBER(S) ARO 23654.28-PH
6a. NAME OF PERFORMING ORGANIZATION Cornell Univ	6b. OFFICE SYMBOL (If applicable)
	7a. NAME OF MONITORING ORGANIZATION U. S. Army Research Office
6c. ADDRESS (City, State, and ZIP Code) Ithaca, NY 14853-2501	7b. ADDRESS (City, State, and ZIP Code) P. O. Box 12211 Research Triangle Park, NC 27709-2211
8a. NAME OF FUNDING/SPONSORING ORGANIZATION U. S. Army Research Office	8b. OFFICE SYMBOL (If applicable)
	9. PROCUREMENT INSTRUMENT IDENTIFICATION NUMBER DAAL03-86-K-0103
8c. ADDRESS (City, State, and ZIP Code) P. O. Box 12211 Research Triangle Park, NC 27709-2211	10. SOURCE OF FUNDING NUMBERS PROGRAM ELEMENT NO. / PROJECT NO. / TASK NO. / WORK UNIT ACCESSION NO.

DTIC
ELECTE
JAN 26 1990
S D
CS

11. TITLE (Include Security Classification)
Search for Far Infrared Radiation from Optically Pumped Defect Modes

12. PERSONAL AUTHOR(S)
A. J. Sievers

13a. TYPE OF REPORT	13b. TIME COVERED	14. DATE OF REPORT (Year, Month, Day)	15. PAGE COUNT
Final	FROM 6/15/86 TO 9/30/89	Nov 13, 1989	58

16. SUPPLEMENTARY NOTATION
The view, opinions and/or findings contained in this report are those of the author(s) and should not be construed as an official Department of the Army position, policy, or decision, unless so designated by other documentation.

17. COSATI CODES		
FIELD	GROUP	SUB-GROUP

18. SUBJECT TERMS (Continue on reverse if necessary and identify by block number)
Far Infrared Radiation; Millimeter Wave Dynamics; Ultraviolet Laser Radiation; Infrared Spectral Hole Burning; Crystal Defects; Optical Photodarkening; Chaleogenide Glasses; Superconductors.

19. ABSTRACT (Continue on reverse if necessary and identify by block number)

A comprehensive experimental study of the near millimeter wave dynamics of a variety of solids is being carried out. Since in many cases the investigation involves driving the system far from equilibrium with IR or UV laser radiation, knowledge of the time dependent optical response over a broad frequency region is required. Effects such as persistent IR spectral hole burning and population inversion in internal vibrational modes in solids have been uncovered using this approach.

(OVER)

20. DISTRIBUTION/AVAILABILITY OF ABSTRACT	21. ABSTRACT SECURITY CLASSIFICATION
☐ UNCLASSIFIED/UNLIMITED ☐ SAME AS RPT. ☐ DTIC USERS	Unclassified
22a. NAME OF RESPONSIBLE INDIVIDUAL	22b. TELEPHONE (Include Area Code) / 22c. OFFICE SYMBOL

DD FORM 1473, 84 MAR

83 APR edition may be used until exhausted.
All other editions are obsolete.

SECURITY CLASSIFICATION OF THIS PAGE
UNCLASSIFIED

The discovery that persistent IR hole burning can be used to manipulate the near millimeter wave response of defects in crystals, such as NO_2^-:KI, and that it also provides a sensitive probe of the optical photodarkening in chalcogenide glasses have opened up new research avenues which require simultaneous probes of very different frequencies in the IR and visible.

On going exploration of the far IR response of high temperature superconductors in sintered, thin film, single crystal and even single grain form continue to provide new information about the dynamical response of these unusual materials both in the normal and superconducting states.

ARO 23654.28-PH

Search for Far Infrared Radiation from Optically Pumped Defect Modes

FINAL REPORT

period: June 15, 1986 through September 30, 1989

A. J. Sievers
Professor
Laboratory of Atomic and Solid State Physics

November 13, 1989

U.S. ARMY RESEARCH OFFICE
DAAL03-86-K-0103

Cornell University
Ithaca, NY 14853-2501

APPROVED FOR PUBLIC RELEASE;
DISTRIBUTION UNLIMITED.

Table of contents

1. ABSTRACT

A comprehensive experimental study of the near millimeter wave dynamics of a variety of solids is being carried out. Since in many cases the investigation involves driving the system far from equilibrium with IR or UV laser radiation, knowledge of the time dependent optical response over a broad frequency region is required. Effects such as persistent IR spectral hole burning and population inversion in internal vibrational modes in solids have been uncovered using this approach.

The discovery that persistent IR hole burning can be used to manipulate the near millimeter wave response of defects in crystals, such as NO_2^-:KI, and that it also provides a sensitive probe of the optical photodarkening in chalcogenide glasses have opened up new research avenues which require simultaneous probes of very different frequencies in the IR and visible.

Our on going exploration of the far IR response of high temperature superconductors in sintered, thin film, single crystal and even single grain form continue to provide new information about the dynamical response of these unusual materials both in the normal and superconducting states.

2. EXECUTIVE SUMMARY

Progress in the understanding of the optical pumping of defect modes, in particular, and the near millimeter wave (NMMW) properties of solids, in general, has been pursued over a wide front during the past three years. One measure of the effort is the 27 published papers, 26 published talks and 4 theses which have been completed.

During this period the new field of high temperature superconductivity was discovered. Since the energy gap for these materials occurs in the middle of the far infrared (FIR) and since the electromagnetic skin depth is ~ 2000A, this technique provides an important window through which to observe the dynamics of these novel materials. The other possible technique, electron tunneling, generates data which has proven to be extremely difficult to interpret because the electrons probe the contaminated surface which is not characteristic of the bulk since the range of the superconducting wave function is comparable to the contamination thickness ~ 10 to 30 A.

From our measurements on sintered material, single crystals and thin films we have been able to show that the intrinsic properties of the high T_c materials are still to be determined. Still the general behavior of the electromagnetic response is understood qualitatively. These materials in the superconducting state do have extremely high reflectivities in the NMMW region but in the IR region the reflectivity is quite small and temperature dependent similar to that of nonsuperconducting ceramic oxides.

Our most recent measurements have been on isolated single crystal grains. The results show that in the superconducting state a giant electric dipole resonance occurs in the NMMW region for $La_{1-x}Sr_xCuO_{4-y}$. The resonant frequency can be tuned throughout this spectral region by simply changing x. These results specify fairly precisely the physical parameters characterizing the response of the system in both the normal and the superconducting states.

A detailed discussion of our investigation into the electromagnetic properties of these superconductors is presented in the Progress Report in Section (3.1). Since the results do confirm that FIR spectroscopy is an important tool, it is proposed that this work

be continued. Continued comparison of theory with experiment for the sintered material is extremely important because at present such theoretical analysis does not give results consistent with the thin film and single crystal data. Since all new high T_c superconductors first appear as sintered pellets this disagreement needs to be understood if the FIR measuements are to reach their full potential.

Persistent IR spectral hole (PIRSH) burning has now been observed for electronic defect states in disordered semiconductors, molecules in dielectric crystals and molecules in semiconducting glasses. We discovered that the excited electronic defect states in ordered semiconductors overlapped each other producing homogeneously broadened transitions which could not be hole burned. Disordered semiconductors, on the other hand, had inhomogeneously broadened transitions which did indeed show persistent effects. Since all internal vibrational modes of molecular defects in crystals are extremely well localized the transitions are inhomogeneously broadened hence such systems are good candidates for high resolution PIRSH burning. The effect has been found for a variety of symmetry types ranging from spherical to diatomic to asymmetric.

The NO_2^-:alkali halide system has proved to be particularly rewarding since a variety of new persistent effects in the IR and the FIR have been discovered. Burning in the IR produced the following results: first, hole burning one part of a tunneling manifold in the vibrational transition produced holes in other parts, second, hole burning one vibrational mode changes the absorption strengths of the other internal vibrational modes and third, the same procedure changes the FIR spectrum of the crystal. This last effect is quite interesting as well as useful since it demonstrates that the properties of the localized phonon modes which involve both the lattice and the molecule are directly coupled to the internal modes of the molecule alone. Finally the internal vibrational modes are also directly coupled to the local axes of the molecule in the lattice. This coupling causes the molecule to reorient while irradiated with weak diode laser radiation at the vibrational resonance frequency. Once reoriented the molecule must overcome a potential barrier to return to the equilibrium configuration. Since this is an activated process, at low

temperatures the recovery is suppressed hence the appearance of persistent holeburning in this system. This technique has been used successfully to determine the equilibrium orientation of the molecule with respect to the crystal axes of the host lattice.

The first attempt to hole burn this defect:lattice system directly in the FIR has been made possible by first identifying all of the isotopes of the gap modes and then fine tuning the mode frequency by alloying another alkali halide with the host lattice. The mode can be shifted to higher or lower frequencies by 0.2 cm^{-1} using this technique of "poor man tuning". No persistent hole burning has been observed. The negative result indicates that either the FIR laser did not have sufficient intensity to determine the low burning efficiency or that the photon energy is too small to put the molecule in the nearly forbidden excited state configuration. Most of Section (3.2) is directed towards explaining these measurements. More work needs to be carried out on FIR holeburning to determine which limit is correct. In addition, our discovery that PIRSH burning occurs in combination bands in the near IR also needs to be examined more systematically.

The discovery of PIRSH burning at molecules in chalcogenide glasses has opened up a completely different kind of persistence mechanism. Now one does not rely on the molecule to produce more than one ground state configuration to support persistent dynamics but instead rearrangement of the disordered lattice itself. The fact that we have observed persistence for molecules which form a chemical bond (HS: inhomogeneous width ~ 200 cm^{-1}) as well as molecules which are simply trapped in the glass upon cooling (CO_2: ~ 5 cm^{-1}) support this statememt. A description of this work is given in Section (3.2.4). It should be noted here that the HS molecule produces a distinct absorption feature in commercial meter long IR fibers made of As_2S_3. With sufficient intensity it should be possible carry out PIRSH burning in the fiber at room temperature even though the persistence time would be extremely small.

A new research direction involves PIRSH's in the chalcogenide glasses as sensitive detectors of atom rearrangements. The investigation involves using the interaction between the photodarkening (PD) of these glasses by band gap radiation and PIRSH generation to

understand PD itself. Because PIRSH burning centers are by their very nature sensitive to changes in their local environment any process which produces long range structural changes in the glassy host should produce measurable changes in the persistent holes. Recently, we have searched for such an effect , and found that extremely large changes in holes can be produced with surprisingly low doses of band gap radiation. We intend to set up an interference pattern with a band gap laser and study persistent hole production as a function of fringe spacing to investigate the range of influence of the photo-induced changes. The results would help decide whether PD is associated with migrating localized defects or the long range rearrangement of many atoms.

In 1988 it was suggested by the PI and his colaborator Professor S. Takeno in Japan that plane wave phonons were insufficient to describe the thermodynamic properties of crystals at finite temperature. It was proposed that in addition to the plane wave modes which minimized the lattice anharmonicity the crystal also contained localized vibrational modes which maximized the crystal anharmonicity. These localized modes move as particles which have an internal vibrational degree of freedom. We call them "anons".

The new feature with respect to the thermodynamic properties of glasses is that they diffuse through the lattice and do not transmit sound like phonons do. We have shown that these modes can account for the unusual specific heat of glasses since the translational diffusive motion produces a linear temperature dependent contribution to the specfic heat and the internal vibrational degree of freedom provides the extra cubic temperature dependence, over an above Debye, both of which are observed in experiments. A more detailed description of these ideas is presented in Section (3.3).

Although we have shown that the presence of anons can describe the low temperature specific heat of glasses, we propose that these particles could exist in doped crystals as well. The localized strain field near an extrinsic defect (such as an ion or a molecule) could act as an anon trap. We are investigating the possibility that the Ag+ impurity in KI:Ag^+ may have such an anon bound to it at low temperatures but that the excitation may be released as the temperature is increased to 20 K. This process could

explain the rapid transformation of the Ag^+ ion from an on-center to an off-center impurity as the temperature is varuied over this limited range.

Another place where a trapped anon may influence experiment is in the incoherent saturation of the internal vibrational modes of molecules in crystals. Exciting the internal mode of the molecule could provide enough local energy to release the anon from the trap site. This extra degree of freedom would provide another relaxation channel besides photon emission or multiphonon emission by which a vibrational quantum could be removed from the molecule.

The arrival of a tunable UV-IR Spectra Physics laser gives us the unique opportunity to pump the electronic and vibrational transitions of different point defects and molecules while at the same time monitoring their translational vibrational spectrum in the NMMW region. One expected effect at low temperatures is persistent UV hole burning. The induced change is expected to alter the impurity induced absorption spectrum in the far infrared. In addition, this pump will permit the localized and resonant vibrational modes associated with the defect to be driven in a controlled manner far from equilibrium.

3. PROGRESS REPORT

3.1 The Electrodynamics of High Temperature Superconductors

3.1.1 Background information

The far-IR properties of the high T_c compounds[1] in sintered polycrystalline, thin film and single crystal form continue to surprise and fascinate solid state spectroscopists in ever increasing numbers. Although the experimental situation is in constant turmoil nearly everyone agrees that in the visible the material is black as coal with a low reflectivity like that of a wide band gap semiconductor while in the far infrared the reflectivity in the superconducting state corresponds to that of a metal not a lossless metal, characteristic of a superconductor at frequencies below the energy gap, but still a good metal. Divining more than this from the data is what continues to produce controversy but, on the other hand, it is also what makes these materials of spectroscopic interest. To appreciate the fundamental IR problems it is useful first to review the electromagnetic response for low temperature superconductors.

In general, a nonlocal relation between the current density and the electric field together with Maxwell's equations must be used to describe the fields inside a pure metal at low temperatures. The surface impedance concept permits a reformulation of the problem in terms of a boundary condition on the fields at the metal surface. The defining equation is

$$\mathbf{E}_t = z\,\mathbf{H}_t \times \mathbf{n} \tag{1}$$

where the subscript t signifies the external tangential fields evaluated at the boundary, the normalized surface impedence $z = Z/Z_0$ with Z_0 the impedence of free space and $\mathbf{n}$ is the normal to the metal surface. The complex coefficient z completely characterizes the medium so the normal incident reflectivity R and the absorptivity A are related by

$$A = 1 - R = \frac{4r}{(1+r)^2 + x^2}. \tag{2}$$

For most metals $r, x << 1$ so that the absorptivity reduces to

$$A = 4r. \tag{3}$$

The absorptivity of a dirty metal in the far infrared corresponds to the classical skin effect limit. In this regime the electromagnetic skin depth δ is large compared to an electron mean free path $v_F\tau$ so that a local conductivity $\sigma(\omega)$ can be defined. If, further, it is

assumed that that the carrier scattering time is independent of energy and that the Drude model can be used to describe the a.c. conductivity then

$$\sigma(\omega) = \sigma_0(1 - i\omega\tau)^{-1} , \quad \sigma_0 = (\omega_p^2 \tau) / 4\pi \tag{4}$$

where σ_0 is the dc conductivity and ω_p is the plasma frequency. Note that two parameters τ and ω_p characterize the electromagnetic properties of the metal. The corresponding components of the surface impedance are

$$r = (1/2\omega_p\tau)(2\omega\tau)^{1/2}[(1 + \omega^2\tau^2)^{1/2} - \omega\tau]^{1/2} \tag{5}$$

and

$$x = -(1/2\omega_p\tau)(2\omega\tau)^{1/2}[(1 + \omega^2\tau^2)^{1/2} + \omega\tau]^{1/2} . \tag{6}$$

In the far infrared, $\omega\tau << 1$ and the absorptivity at normal incidence has the simple Hagen-Rubens form

$$A_n(\omega) = (2\omega / \pi \sigma_0)^{1/2} \tag{7}$$

in which A_n increases as $\omega^{1/2}$. At a frequency of 100 cm^{-1} and a resistivity of 70 $\mu\Omega$cm, $A_n = 0.03$. For larger infrared frequencies, in the limit where $1 << \omega\tau << \omega_p\tau$, the absorptivity has the constant value

$$A_n(\omega) = 2 / (\omega_p \tau) . \tag{8}$$

At still larger frequencies, in the visible, transitions to other bands become important and the simple intraband absorption model given here is no longer applicable.

For materials with small conductivities the high frequency interband transitions can still influence the the size of the absorptivity in the IR and FIR region through their effect on the displacement current in the medium. This effect can be seen most easily when the dielectric function of the medium $\varepsilon(\omega)$ is written in terms of the contribution from the displacement and conduction currents so

$$\varepsilon(\omega) = \varepsilon_\infty + 4\pi i \sigma(\omega)/\omega \tag{9}$$

where ε_∞ is the constant low frequency contribution from the interband transitions. When this contribution is significant it is often useful to plot $\sigma_1(\omega)$ and $\varepsilon_1(\omega)$ rather than $\sigma_1(\omega)$ and $\sigma_2(\omega)$ so that the two Drude parameters τ and ω_p will be evident. If the material has a magnetic response as well as an electric one then to compare theory and experiment in the local limit, the connection between the surface impedance and the different susceptibilities is

$$z = [\mu(\omega)/\varepsilon(\omega)]^{1/2} \quad . \tag{10}$$

The dotted curve in Fig. (1) shows the measured surface resistance at room temperature for an annealed lead foil in the far infrared spectral region[2]. A multiple parallel plate waveguide technique was employed to measure this small absorptivity. In this frequency region the displacement current is negligible compared to the conduction term and also $\mu = 1$. The solid curve in the figure is calculated from the Drude theory with the measured dc conductivity of the foil inserted into Eq. (7). With no free parameters good agreement is obtained between theory and experiment throughout this spectral region.

Because of Landau damping the FIR absorptivity of a pure metal at low temperatures no longer agrees with the simple Drude predictions based on a temperature dependent relaxation time. This anomalous skin effect regime has been well studied both

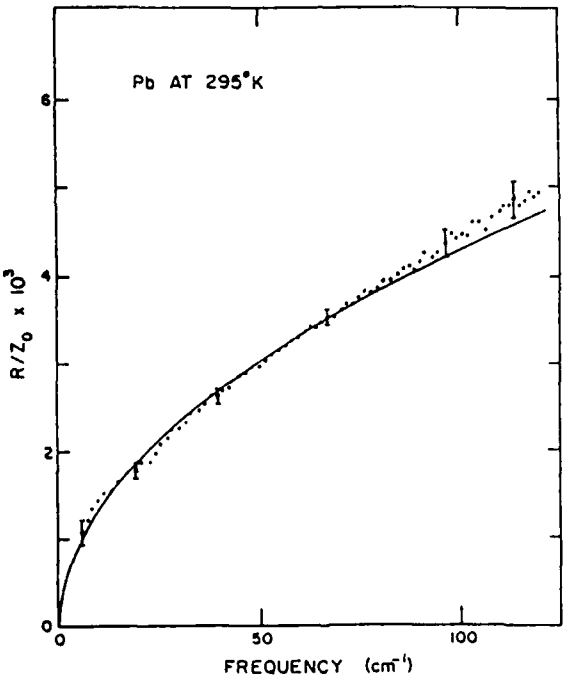

Figure 1.

in the normal state and in the superconducting state. The frequency dependent response of a superconductor in the extreme anomalous limit as calculated by Mattis and Bardeen[3] is shown in Fig. (2). The electromagnetic gap $\hbar\omega_g = 2\Delta = 3.5\ k_B T$ for this weak coupling limit. The normal state conductivity σ_n is assumed to be entirely real in this frequency interval ($\omega\tau << 1$) and the results are shown as a ratio of the real σ_1 and imaginary σ_2 in the

superconducting state to σ_n. These conductivity expressions also apply in the opposite or extreme dirty limit. The ratio of the extreme anomalous surface resistance in the superconducting state to the normal state for a bulk sample is also shown in Fig. (2). For the opposite limit Tinkham[4] has shown that the frequency dependence of the surface resistance remains qualitatively the same as in Fig. (2).

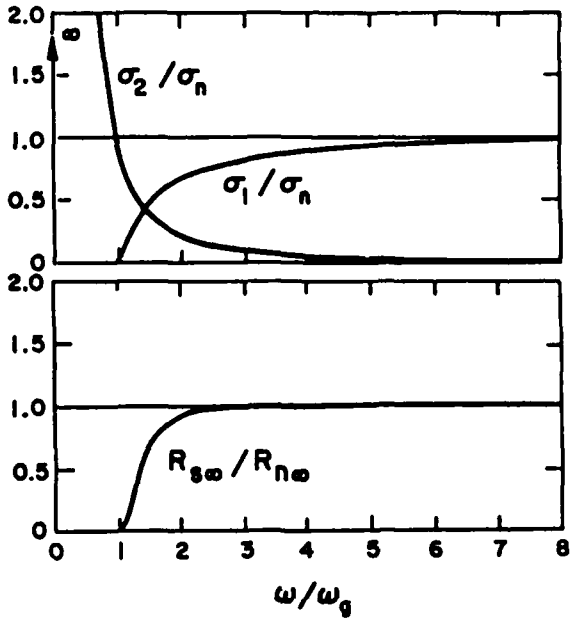

Figure 2.

For a strongly coupled superconductor such as Pb the spectrum for the superconducting state is made complex by the appearence of the Holstein absorption process[5-8]. The coupling between electrons and phonons in metals makes allowed an infrared absorption process at low temperatures associated with phonon generation by the excited electrons. The product of the square of the electron-phonon matrix element and the phonon density of states in the metal can be obtained from a measurement of the difference in the FIR absorptivity between the superconducting and normal state.

Measurements[9] of the difference in the FIR surface resistance between super and normal for the extreme anomalous (Pb) and the extreme dirty (Pb-0.1In) limits are shown in Fig. (3). Above the gap frequency the absorptivity in the superconducting state exceeds that in the normal state up to frequencies about 10 x the gap frequency. Note that the alloy sample has a much larger surface resistance in the normal state below the gap than does the pure Pb sample and that it also has a corresponding larger surface resistance in the superconducting state above the gap. These results illustrate the "Brändli sum rule" that the

absorptivity in the normal state below the gap must equal the excess absorptivity in the superconducting state above the gap[9], i.e.,

$$\int_0^\infty r_s(\omega)\, d\omega = \int_0^\infty r_n(\omega)\, d\omega \ . \qquad (11)$$

Another interesting feature about the data shown in Fig. (3) is that the frequency dependence of the excess absorptivity in the superconducting state is completely different for the two cases. For pure Pb the profile is associated with the availablility of phonons hence for T = 0 with the spectrum of the phonon density of states whereas for the alloy case the main ingredient is quasi-elastic scattering near zero frequency.

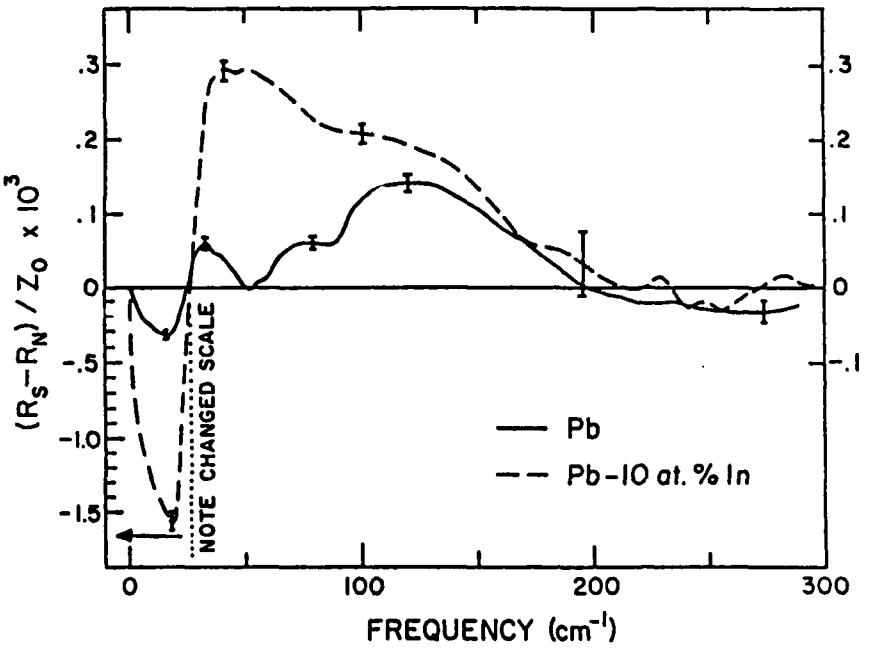

Figure 3.

3.1.2 High T_c sintered Samples

The room temperature FIR reflectivity of sintered polycrystalline $YBa_2Cu_3O_{7-y}$ is represented by the solid line in Fig. (4a)[10]. The classical skin effect prediction (dashed line)for a dc resistivity of 800 μΩcm (the measured resistivity is 890 μΩcm ± 10%) is also shown. At the lowest frequency limit of our data the two curves converge, but for higher frequencies, the reflectivity deviates strongly from the Drude prediction. We also observe very little temperature dependence to the reflectivity (100 K, dotted line) in agreement with other measurements at larger frequencies. While the dc resistivity changes by a factor of three from just above T_c to room temperature, the reflectivity changes by only a few

percent[10].

Figure (4b) shows the room temperature reflectivity as a function of frequency on a logarithmic frequency axis, covering four decades in frequency. These results are similar to those reported by others[11-13]. The appearance of phonon modes such as those shown in the 100 to 1000 cm^{-1} region is not common in metallic reflectivity, but they have been seen in materials with small optical conductivity[14].

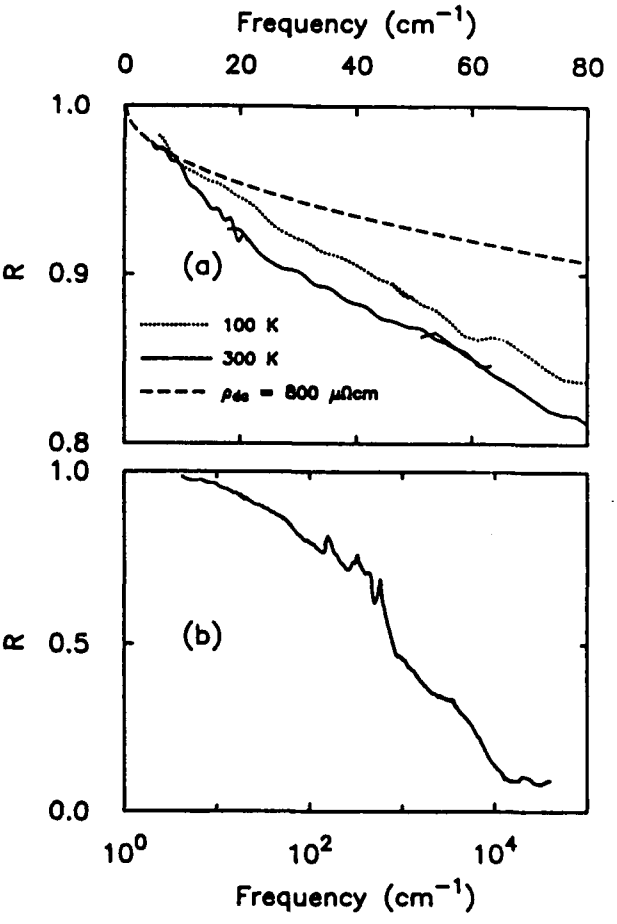

Figure 4.

How can one analyze such sintered material data more quantitatively? With the definitive observation[15] in the FIR reflectivity of 2-dimensional optical conductivity in the ab plane of single crystal La_2NiO_4, a compound structurally isomorphic to $La_{1.85}Sr_{0.15}CuO_{4-y}$ (the 40 K superconductor), an effective medium modeling of the FIR data for both the superconducting and normal state of the sintered material becomes practical. For the grain size small compared to the wavelength and for 2-D conduction with the third direction in the grain insulating, the effective medium approximation (EMA) equation has a relatively simple form, with a fixed fill fraction of f = 2/3 for the metallic component. To make the problem tractable we have assumed that the crystallites are

spheroids with the same symmetry as the conductivity tensor, so that a single parameter, the depolarization factor, L, along the c direction of the crystallite, specifies the EMA. The effective conductivity for the medium is obtained by solving the following equation[16]:

$$\frac{2}{3}\frac{\sigma_{a,b}-\sigma_e}{(1+L)\sigma_e+(1-L)\sigma_{a,b}}+\frac{1}{3}\frac{\sigma_c-\sigma_e}{2[(1-L)\sigma_e+L\sigma_c]}=0 \qquad (12)$$

where σ_e is the desired conductivity of the isotropic effective medium in terms of the known conductivities of the individual anisotropic grains.

For the case of spherical crystallites, L = 1/3 and Eq. (12) reduces to the standard EMA result for an anisotropic polycrystalline material. For needle-like crystallites L = 0 along the c axis, while for plate-like crystallites L = 1. We find that this EMA with Lorentz oscillator contributions for the phonons and a two dimensional Drude free carrier component provides a good description of the normal metal results for the sintered systems throughout the FIR region[16,17].

Figure 5(a) presents our FIR data on the reflectivity of $La_{1.85}Sr_{0.15}CuO_{4-y}$ in the normal state (T = 40 K, dashed curve) and in the superconducting state (T=10 K, solid curve)[10]. The dashed line fit shown in Fig. 5(b) demonstrates that the Drude term does not provide enough reflectivity at low frequencies. The calculated reflectivity for the superconducting state represented by the solid line in Fig. 5(b) makes use of the Mattis-Bardeen equations to model the 2D superconductivity in the a,b plane. This too reproduces some of the qualitative features observed in Fig. 5(a), for example, although 2D is chosen as 68 cm^{-1}, the onset of absorption occurs at about 35 cm^{-1}. Also the reflectivities cross at 73.7 cm^{-1} and the normal state becomes more reflecting than the superconducting state above this frequency.

To demonstrate the key role of grain geometry, Fig. 5(c) shows the reflectivity in the superconducting and normal states as calculated with the EMA using identical parameters as Fig. 5(b), except that L_c = 0.7, corresponding to oblate spheroids. Immediately obvious is the dramatic loss of the enhanced absorptivity in the superconducting state above the gap and the shift in position of the equal reflectivity frequency which often has been associated with the frequency of the energy gap, 2Δ.

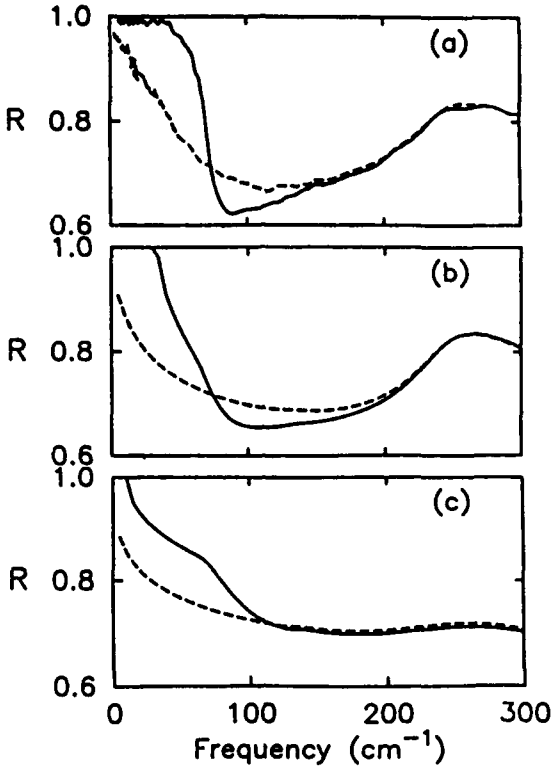

Figure 5.

The qualitative agreement between the EMA calculations and the measured reflectivity on the sintered material in the long wavelength limit demonstrates that the individual grains are highly anisotropic in the far infrared spectral region. The good specular properties of the sintered samples in the visible indicate that the grains must be nearly isotropic at these wavelengths. Between these two limits the grain size is comparable to the wavelength of the radiation and the grains are anisotropic so that the surface appears rough and scatters radiation. So far there is no theory to describe the results in this region.

3.1.3 Optical Properties of composites

Recently there has been much controversy surrounding the origin and significance of a peak centered around 0.5 eV in the optical conductivity of sintered high temperature superconductors. Several reports[18,19] have been published on the IR spectrum of sintered $YBa_2Cu_3O_{7-x}$ and $La_{2-x}Sr_xCuO_4$ which claim that the observed correlation between the oscillator strength of the "0.5 eV" peak and the degree of "superconductivity" in the samples might indicate that pairing in these materials is mediated by a high-energy electronic excitation such as an exciton[20]. Later, IR measurements of single crystals

were made by many workers, using both reflectivity[21,22] and direct absorption methods[23]. Most of these measurements on single crystals have failed to show a strong "0.5 eV" peak although a broad absorption is observed to extend throughout the IR spectral region. Figure (6) shows an IR peak in the conductivity for three different sintered copper oxide compounds. The top trace is for the 40 K superconductor, the middle trace is for the 90 K superconductor and the bottom trace is for a non-superconductor[24]. The compound $La_4BaCu_5O_{13}$ can be viewed as a cubic perovskite with an array of channels of oxygen vacancies running parallel to the c axis, so the Cu-O network is three dimensional but anisotropic[25]. The 3-D conductivity screens the phonon dipole moments and keeps the lattice component from showing up even in the sintered pellets.

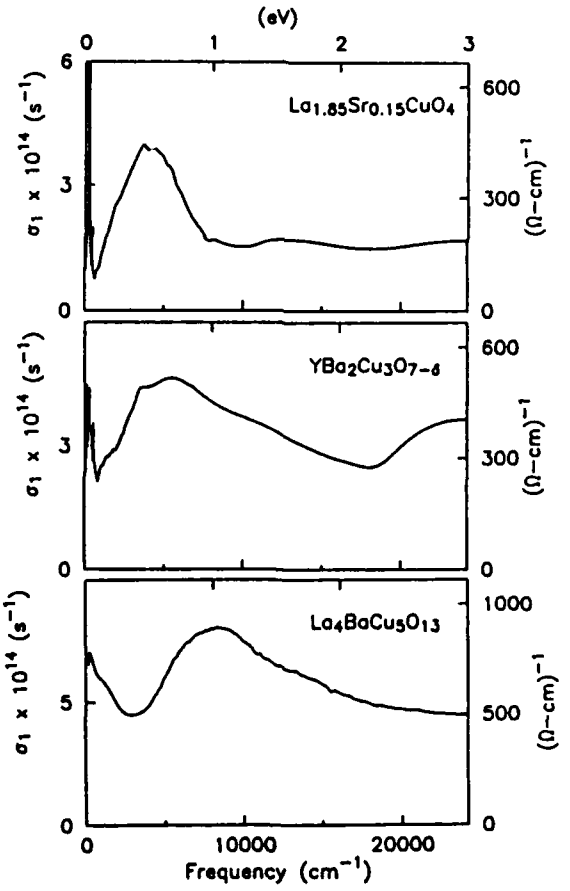

Figure 6.

Why the "0.5 eV peak" appears in the sintered copper-oxide perovskite-like materials is an interesting question even if it is not an intrinsic effect. Possible answers

could involve: (1) effects of the composite nature of the system such as sphere resonances; or (2) the strong anisotropic nature of the material and the random orientation of the grains. In a recent Comment, Orenstein *et al.*,[26] proposed a simple model which explains the "0.5 eV absorption peak" in terms of the optical anisotropy of the material in the geometrical optics limit. While this model seems to reproduce qualitatively the presence of the peak in the mid-IR, we believe that the complete picture must be more complicated. In this region of the spectrum, the size of the anisotropic grains is such that neither the geometrical nor effective medium limits can be correct, and scattering effects must be important. It may be that the origin of the peak can be determined more clearly by careful studies in which the grain size and porosity of the materials can be controlled.

3.1.4 Films and Single Crystal Oxide Superconductors

It is useful to compare the superconducting response of sintered, thin film and single xtal FIR materials. Shown in Figure 7(a) is the ratio of the reflectivity of sintered $YBa_2Cu_3O_{7-y}$ in the superconducting state (10 K) to that in the normal state (100 K). The polycrystalline nature is accounted for again with the EMA[27]. The dashed curve in Fig. 7(a) is obtained from such a fit to the normal state data, followed by the application of the MB equations to model the free electron conductivity. Here a gap of 170 cm^{-1} was obtained for plate-like crystallites. An equally satisfactory fit is obtained with a gap of 150 cm^{-1} for spherical crystallites. The relative superconducting gap energies obtained from sintered sampes of both $YBa_2Cu_3O_{7-y}$ and $La_{1.85}Sr_{0.15}CuO_{4-y}$ are thus seen to be similar, with $2\Delta/kT_c = 2.6$.

Contrasting with the behavior of the bulk samples, Figure 7(b) shows data for 1 μm thick films of $YBa_2Cu_3O_{7-y}$ on ZrO_2. These films are of high quality, having $T_c = 85$ K and $J_c > 10^6$ A/cm^2 at T= 4.2 K. The films are somewhat oriented, with the c-axis preferentially perpendicular to the film surface. Using the same dielectric function in the a-b plane obtained from fitting the data on bulk material, but with the measured dc resistivity of 200 μΩcm in the a-b plane, produces the dashed curve in Fig. 7(b). Here the choice of the gap energy indicates $2\Delta/kT_c = 6.4$, larger than the value obtained for bulk sintered material. The conductivity obtained from a Kramers-Kronig transformation of the reflectivity covering over three orders of magnitude in frequency does not show the

electronic mode in the IR found for bulk polycrystalline samples.

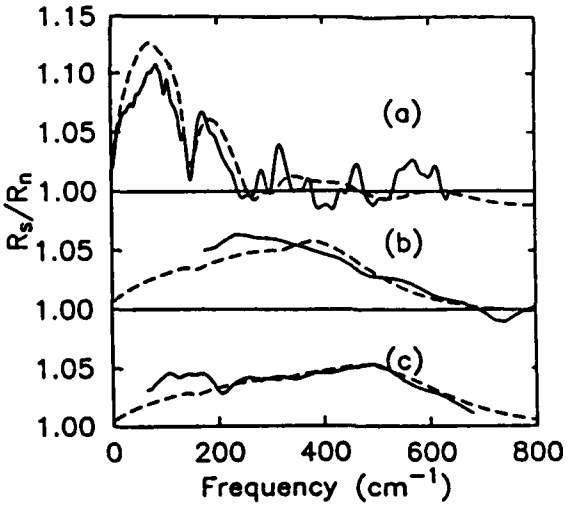

Figure 7.

Just as the relative gap parameter for the films exceeds that of the sintered material, so that of the single crystals exceeds that of the films. Single crystals have been pieced together to form a mosaic with the c-axis normal to the surface. Our reflectivity measurements shown in Fig. 7(c) and our determination of the gap parameter, $2\Delta/kT_c = 8$, are in agreement with those reported on single crystals by others [21]. Again the dashed curve is a fit to the data using the dielectric function determined on the bulk, with a dc resistivity of 200 $\mu\Omega$cm. The gap value is determined from this fit. As for the films, the reflectivity signature of the superconducting state is not "complete" in that there is absorption of energy below 2Δ. Thus the dashed curve in Fig. 7(c) has been reduced by 50% to agree with the overall magnitude of the data. Our measurements on different single crystals show that this absorption below the gap is not the same from sample to sample hence it must be an extrinsic effect.

Recently Timusk *et al.*,[28] proposed an alternate explanation for the R_s/R_n results which does not make specific use of a gap or equivalently assumes that $\tau^{-1} << 2\Delta$ so that the entire free carrier $\sigma_1(\omega)$ profile in the normal state is compressed into the delta function at $\omega = 0$ in the superconducting state. With τ^{-1} small and $\sigma_1(dc)$ known for the normal state, the conductivity sum rule gives a small plasma frequency. From Hall measurements[29] an estimate of the density of free carriers can be obtained independently.

This value together with the small plasma frequency implies a large carrier mass; however, specific heat gives a carrier mass which is not particularly heavy[30]. At present all of these results do not give a consistent picture.

Currently the far infrared (FIR) spectroscopic data on high T_c single crystals in the superconducting state can be interpreted as evidence for a large energy gap[31], a BCS-like gap[32] or no gap at all[33]. The optical properties of crystals of variable quality make it difficult to conclude whether or not the peak observed in the ratio of the FIR reflectivity of the ab plane of $YBa_2Cu_3O_{7-y}$ in the superconducting state to that of the normal state should be interpreted as evidence for the energy gap[31,32] or as evidence for a zero crossing of the real part of the dielectric function[33]. The gap of $La_{2-x}Sr_xCuO_{4-y}$ is even less well determined because it has been difficult to grow single crystals at the Sr doping which produces the highest T_c's. The optical properties of superconducting sintered $La_{2-x}Sr_xCuO_{4-y}$ have been analyzed in some detail[34] but the excess absorption in the superconducting state associated with transport between grains obscures the determination of a true gap signature. Compared to the extensive work on these polycrystalline[34,35] or single crystal samples[31-33], the FIR electrodynamics of high T_c superconductors in the isolated particle form have been ignored even though the relation between the bulk dielectric function and the small particle response is well known and has been investigated for many materials[36].

3.1.5 Isolated Superconducting Particles

Our most recent investigation has focused on the FIR response of small isolated $La_{2-x}Sr_xCuO_{4-y}$ particles in the normal and superconducting states[37]. A far infrared superconducting sphere resonance polarized along the c-axis has been observed to decrease in frequency with increasing temperature, increasing magnetic field or decreasing Sr doping. No corresponding resonance is found in the normal state. These observations indicate that an energy gap does exist in high T_c materials since the energy gap frequency must be larger than the c-axis sphere resonance value. These results will be described by Dr. Noh in an invited paper at the March"Solid State" meeting of the American Physical Society.

Before turning to the experimental data we summarize the different kinds of spectral signatures which can be expected to occur for small conducting particles. Let us consider

two specific examples to identify qualitatively the spectral signature for superconductors in small particle form. Assume that a BCS energy gap separates the superconducting ground state from the single particle excited states, that $\omega_p\tau >> 1$ and that either $(2\Delta)\tau >> 1$ or $(2\Delta)\tau << 1$ for a bulk low temperature superconductor. For the first case the entire normal state conductivity spectrum collapses into the delta function at zero temperature with strength $A_I = \int \sigma_n(\omega)d\omega = \omega_p^2/8$. For the second case, $\sigma_1(\omega)$ is zero up to a gap frequency 2Δ, above which it rises monotonically to the frequency independent conductivity of the normal state, σ_n, since ω is still $<< \tau^{-1}$. The strength A_{II} of the $\delta(\omega)$ term comes from the missing area below the gap frequency[38], i.e., $A_{II} \approx 2(2\Delta)\sigma_n$. We show the expected results for the corresponding sphere resonances for these two cases at the top of Table 1 and below those the results for other possible sets of parameters. Depending on the relative size of ω_p, τ^{-1}, and 2Δ, various sphere resonance signatures can be expected in small metallic particles in the normal and superconducting states.

Table 1.

Case	Conditions	Observable? (normal)	(s.c.)	Characteristics
I	$\omega_p\tau >> 1$, $(2\Delta)\tau > 1$	yes	yes	The line width will narrow drastically upon cooling below T_c.
II	$\omega_p\tau >> 1$, $(2\Delta)\tau << 1$	yes	yes	The line width will not change upon cooling below T_c.
III	$\omega_p\tau \leq 2$, $(2\Delta)\tau > 1$	no	yes	The peak position will not have a strong temperature dependence.
IV	$\omega_p\tau \leq 2$, $(2\Delta)\tau << 1$ and $\omega_{sr} < 2\Delta$	no	yes	The peak position will have a strong temperature dependence.
V	$\omega_p\tau \leq 2$, $(2\Delta)\tau << 1$ and $\omega_{sr} >> 2\Delta$	no	no	The peak will be overdamped since $\mathrm{Im}\{\varepsilon(\omega_{sr}) + 2\varepsilon_h\}$ is large for both states.

The FIR temperature dependence of the absorption coefficient, α, for 1% $La_{1.85}Sr_{0.15}CuO_{4-y}$ in Teflon is shown in Figure (8a). The absorption coefficient difference $\Delta\alpha(T) = [\alpha(T) - \alpha(T=40K)]$ is plotted versus temperature. The low temperature absorption peak, located at 54 cm^{-1}, shifts to smaller frequencies and weakens as the temperature approaches T_c. No resonance is seen in the normal state. At the resonant frequency the absorption in the superconducting state is larger than the absorption in the

normal state but far from the resonance the reverse is true. A six T magnetic field was observed to decrease the line strength by about 40% and produce effects similar to those obtained with increasing temperature. These observations, which are consistent with Case IV in Table 1, indicate that the resonance is associated with the appearance of superconductivity.

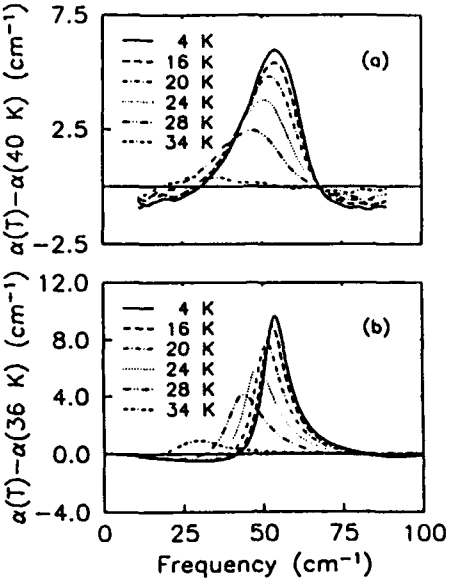

Figure 8.

The Sr concentration dependence and hence the conductivity dependence of the absorption feature is shown in Figure (9). Since the absorption for the same material between 0.3% and 3% fill fraction scales with f, the difference between the absorption coefficients in the superconducting and normal states are normalized by the fill fraction, f, of the superconductor. The peak position and the linewidth of the absorption line increase monotonically with x. However, the normalized absorption value at the peak position and the strength of the resonant feature increase at low concentration of Sr but reach a maximum around x=0.18. Our samples with x=0.225 and 0.25 show no absorption lines up to 180 cm^{-1}, although they are superconducting. Also, no line is observed in non-superconducting x=0.02 and x=0.04 samples.

The general behavior of the peak position and strength as a function of Sr concentration can be explained as a change in the value of σ_n. If σ_n along the c-axis increases with Sr doping like the d.c. conductivity of sintered materials, the position and the strength of the resonance should increase. The disappearance of the resonant feature

above x=0.225 probably results from the resonant frequency becoming much higher than 2D, so that the limit of Case V in Table 1 is in effect. The lack of a resonant feature below

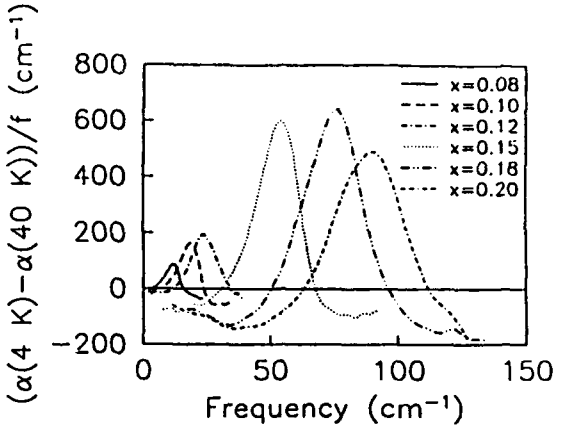

Figure 9.

x=0.04 is due simply to the lack of superconductivity in those samples.

In summary, we have observed a unique resonance phenomenon in well dispersed superconducting $La_{2-x}Sr_xCuO_{4-y}$ particles in teflon. The observed strength and position of the resonance identifies for the first time the value of the c-axis conductivity for large Sr concentrations. The observed behavior of the resonant feature fixes the inequalities that the normal free carrier and superconducting parameters must satisfy, namely, the normal state carriers along the c-axis are heavily damped and the c- axis energy gap frequency is larger than the sphere resonance frequency but smaller than the normal state carrier scattering rate.

All of the data presented here show that the FIR properties of the high T_c superconductors do not correspond to the low temperature ones described in the background section. The sintered Cu-0 materials can be described fairly acurately with the EMA but the sphere resonance results indicate that the derived gap value is too small. At higher frequencies, the IR peak in the effective optical conductivity of the sintered materials is an interesting effect which occurs in a region of the spectrum where composite media analysis is not valid. The IR peak in the conductivity does not appear to be intimately connected to superconductivity since it appears in both superconducting and normal Cu-O materials. A detailed analysis of the single crystal data is still complicated by the variability

of the materials and by the as yet to be determined influence of the heavily twinned a,b plane on the optical constants. In principle, the influence of this single crystal twinning (on the scale of 1000 A) on the IR and FIR properties could be described with still another composite medium representation.

3.2 Optically Pumped Defect Modes in Dielectric Solids

3.2.1 Hole burning history

The formation of persistent spectral holes in electronic bands in solids was first observed in 1974 and at present persistent features caused by both photochemical and nonphotochemical processes continue to be found in an ever increasing number of solids[39]. In the last few years persistent IR hole burning has been observed in the vibrational spectrum of molecular defects in crystals, i.e., no electronic excitation is involved and only vibrational degrees of freedom are photoexcited with IR radiation[40-45].

Persistent IR spectral holes provide a new high resolution technique with which to explore the properties of defects in solids. The inhomogeneously broadened absorption lines associated with the vibrational modes of matrix isolated molecules are in general not coincident with the frequencies of ir-line tunable gas laser : consequently, the high power techniques of incoherent saturation and transient hole burning cannot be applied to identify the dominant relaxation process in most molecular-defect-lattice combinations. With low power tunable diodes two techniques are potentially available: vibrational fluorescence, which gives the excited state lifetime; and persistent hole burning which not only provides a high resolution probe of the defect but also identifies the excited state dephasing time of the vibrational mode.

What are the most general requirements for the formation of persistent IR spectral holes (PIRSH's) that last much longer than excited vibrational state lifetimes at low temperatures? In a general sense, the basic requirements for PIRSH formation are three. First, there must be several ground state configurations of the total system, and the IR energies from these ground states must differ by more than the laser linewidth. Second, there must exist an IR pumping pathway that connects these ground state configurations. Finally, the relaxation among the ground states must be slower than the excited state lifetime. If all of these conditions are met, persistent spectral holes may result.

To date persistent IR spectral holes have been found in solids with three different kinds of bonding: van der Waals[40], ionic[41-43] and covalent[44,45] These new high resolution measurements are attracting widespread interest not only because they

complement earlier results obtained with other spectroscopic techniques on defects in solids but also because the source of the persistence is often not understood. A brief description of persistent spectral hole burning results in the vibrational spectrum of CN^- and NO_2^- in alkali halide crystals and HS in As_2S_3 is given below.

3.2.2 CN^- in alkali halide crystals

Figure 10 shows the low temperature absorption coefficient in the stretch mode frequency region for a KBr crystal doped with 0.05 mole % KCN. The vertical dashed line in the figure divides the spectrum up into two frequency intervals. The absorption lines which occur at frequencies larger than 2100 cm^{-1} are associated with different isotopes of the linear NCO^-, a common impurity in the KCN dopant. The linewidths of these transitions are all about 0.05 cm^{-1} (FWHM). None of these features show spectral hole burning.

The absorption lines at frequencies below 2100 cm^{-1} in Fig. 10a are all associated with the CN^- stretch vibration in some way or other and the complexity of this spectrum is quite surprising. The fine structure near the main ($^{12}C^{14}N^-$) absorption line can be seen more clearly in Fig. 10b where the spectrum of a lower concentration sample (0.01 mole % KCN) is displayed. This spectrum is characterized by one strong central line with a large linewidth (~ 0.2 cm^{-1} FWHM) surrounded by lines which have much narrower linewidths (~ 0.04 cm^{-1} FWHM). In the figure these satellite lines are labelled α_1, α_2, γ_1, γ_2, γ_3 and γ_4. Our hole burning measurements[42] indicate that both the central line and related broad structure should be attributed to tunneling CN^- and the ultrasharp lines, to

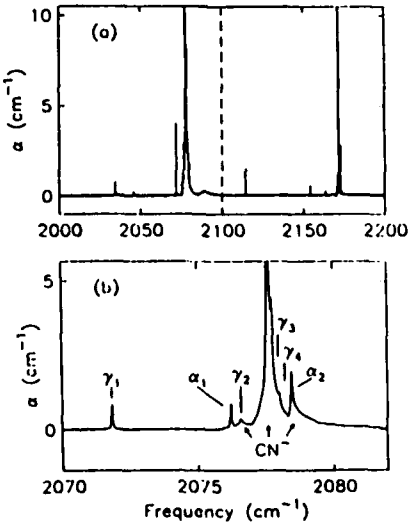

Figure 10.

CN^- molecules frozen in direction by other nearby impurities in the crystal.

No hole burning has been detected in the main line shown in Fig. 10b but the sharp lines labelled α_1 , α_2 , γ_1 , γ_2 , γ_3 and γ_4 all show persistent changes when probed with a diode laser. Examples of hole burning in the three absorption lines α_1 , α_2 , and γ_1 are shown in Fig. 11. Figure 11a shows a hole burned in the α_1 line which can made 100 % deep but which washes out after about three minutes in the dark. The lines γ_2 , γ_3 and γ_4 (not shown) display a similar erasing behavior. Only a shallow hole can be burned in the α_2 line [shown in Fig. 11b] which erases in about 30 sec. Figure 11c shows the γ_1 mode before and after two holes have been burned in it. These holes which can be made 100% deep have the interesting property that they are permanent as long as the sample is maintained at liquid helium temperatures.

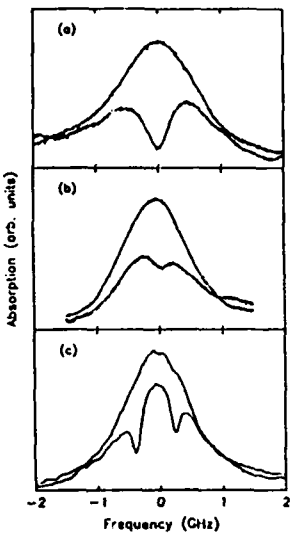

Figure 11.

The temperature stability of the holes burned in the γ_1 band has been determined by sweeping the spectrum with a low intensity probe beam while the sample temperature is varied. Scans at four different temperatures are shown in Fig. 12: trace (a) of a sample at 1.7 K displays a spectrum which contains two holes, trace (b), the same sample at 15 K, trace (c), at 25 K and trace (d), at 35 K. At this highest temperature the spectrum appears nearly featureless yet upon recooling to 1.7 K the original spectral shape is recovered. Erasing does not become noticeable until the sample temperature is cycled up to about 48 K.

A systematic study of crystals double doped with CN^- and with different cation and anion dopants demonstrates that the vibrational center which produces the γ_1 band is a CN^-

molecule with a near neighbor Na^+ impurity replacing one of the K^+ host ions[42]. Other

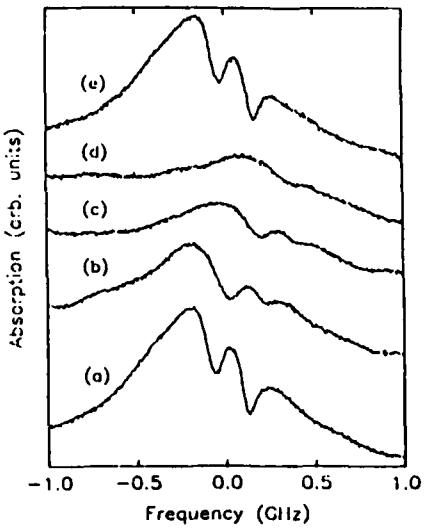

Figure 12.

complexes consist of the CN^- molecule together with an alkali or halogen ion impurity at a nearby lattice site. Of the fourteen new centers identified, six of them show persistent hole burning when the perturbed CN- stretch mode is probed with a low power diode laser. The extremely stable defect complex: CN^-: Na^+, which both fluoresces and hole burns, has been investigated in some detail. By combining broadband Fourier transform interferometry with narrow band diode laser hole burning it has been demonstrated that the particular persistent effect associated with the γ_1 band occurs when, during vibrational de-excitation, the CN^- molecule flips by 180° between inequivalent energy configurations generated by the presence of the nearby Na^+ ion.

3.2.3 NO_2^- : the asymmetric top defect

When the nitrite molecule NO_2^- is doped into single crystal KI a number of spectral features appear in the gap region of the pure crystal phonon spectrum which have remained unexplained for a quarter century. These excitations, which have been studied by direct far infrared (FIR) absorption[46-48], infrared (IR) sideband absorption[49], Raman scattering[50-53], ultraviolet (UV) absorption[53,54] and emission[55], have been attributed to some combination of translational modes and/or librational modes of the molecule but no asignment is consistent with all the available spectroscopic data nor have the gap mode features ever been resolved.

A new solid state high resolution spectroscopic technique has been developed to

provide information about the source of the gap mode features in the KI: NO_2^- system: it involves PIRSH burning in the IR while probing concommitant changes in the FIR. Initially, tunable infrared diode lasers are used to burn persistent IR spectral holes (PIRSHs) in the internal vibrational spectrum of NO_2^- defects in KI at low temperatures through a reorientational form of hole burning. Next, the technique of PIRSH burning in the internal bending mode of NO_2^- is combined together with high resolution FIR fourier transform interferometry to probe simultaneously the KI:NO_2^- gap features. We find that persistent polarized changes in the FIR spectrum are coupled to persistent changes in the internal vibrational mode spectrum but the production of persistent holes in the IR does not translate into FIR holes in the external modes. The results show that the three FIR absorption lines in the gap are consistent with localized translational motion of the NO_2^- ion[43].

The experimental arrangement for probing the crystal simultaneously with the diode laser pump beam and the FIR interferometer probe beam is shown in Fig. (13). FIR transmission spectra are obtained with a Bomem interferometer with a maximum apodized resolution of 0.004 cm-1 (120 MHz). The interferometer is configured with a Hg arc source, 12 mm mylar beam splitter, and a Si composite bolometer at 4.2 K. The interferometer beam is focused into a sample located in a superfluid He immersion optical access cryostat (not shown). The laser polarization is rotated to any angle using a quarter wave plate and linear polarizer. Efficient illumination of the 1.5 x 5.0 mm sample face seen by the IR beam is accomplished with a ZnSe cylindrical lens. Metal film attenuators are

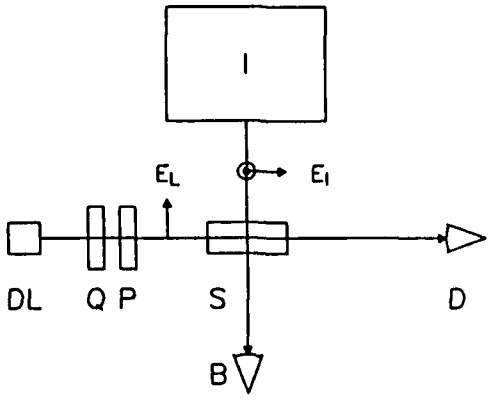

Figure 13.

used to decrease the laser intensity after burning so that the persistent hole shape can be monitored without distortion. Verification of proper IR sample illumination and monitoring of the persistent spectral hole is provided by a HgCdTe or a Ge:Cu detector.

Figure (14) shows the PIRSH burning effects that can be produced with a low power diode laser in the ν_2 (A1 symmetry) infrared bending mode of NO_2^- at 804.85 cm^{-1}. Curve (a) is the undistorted absorption band as measured in transmission by tuning the attenuated laser beam through a few GHz about the line center. To burn a hole, the laser frequency is returned to the center of the absorption band and held fixed. At the highest intensities used (25 mW/cm^2) the absorption at the laser frequency decreases to zero in about ten seconds. In the dark this absorption hole decays roughly exponentially with a decay time of 50 minutes at 1.5 K. Holes burned with an intensity less than 0.2 mW/cm^2 cannot be burned 100% deep, and no detectable hole is burned with an intensity less than 2 mW/cm^2. The hole shown in Fig. (14), curve (b) is about 200 MHz wide only because the hole is 100% deep. Note that although antihole wings appear they are much too small to account for the missing area associated with the appearance of the spectral hole. Holes as narrow as 37 MHz have been burned in this band in the low intensity, short burn time limit.

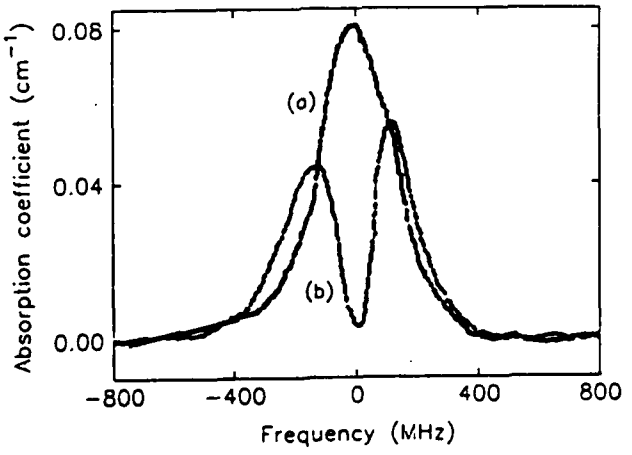

Figure 14.

The PIRSH burning process is summarized as follows: The laser excites the vibrational bending mode of an NO_2^- ion originally in one of the 12 allowed orientations. During de-excitation an ion reorients with low probability (~ 10^{-2}) to one of its other 11

positions. Three of these preserve the dipole axis (not necessarily direction), and these three antihole positions appear in the same polarization. The other 8 positions have their permanent dipole directions orthogonal to the starting direction. The long time branching ratios for reorientation appear to be roughly equal. Barriers to reorientation at 1.5 K allow the molecular ions to remain in a nonthermal equilibrium distribution of orientations for an extended period of time after the burning process. Since PIRSH burning effects have never been investigated in the FIR, we now proceed to examine the effect on the gap mode spectrum of KI:NO_2^-.

The low temperature absorption spectrum of KI:NO_2^- in the gap mode region at an interferometer resolution of 0.015 cm^{-1} is shown in Fig. (15a). The doublet, which is resolved here for the first time, increases the number of known strong IR active NO_2^- modes in the gap from two to three. In addition, each mode is found to have a weak low frequency shoulder consistent with an isotope shift due to the 7% abundant ^{41}K isotope in the KI host.

When the internal bending mode is IR hole burned, the FIR spectrum changes and these results are summarized in Figures (15b) and (15c). In the arrangement shown in Fig. (13) , the diode laser beam is unblocked and an IR hole is burned in the ν_2 mode. After 30 minutes of burning at an intensity of about 0.2 mW/cm^2 to reach a steady state hole, the FIR spectrum is obtained with an integration time of about an hour at a resolution as high as 0.015 cm^{-1} (450 MHz) as determined from the width of low pressure water vapor lines. Next the diode is blocked and the sample is warmed to 10 K to erase the hole, cooled to 1.5 K again and an FIR reference spectrum is obtained. Ratioing the burned to the unburned sample spectra reveals the absorption coefficient changes for the NO_2^- molecule shown in the figure. The changes produced in these external modes do not display sharp holes but instead consist of line strength changes over the entire FIR lines. Erasing the entire IR bending mode in each of these experiments only increases the strength of these FIR changes. In Figures (15b) and (15c) the laser polarization is configured either parallel or perpendicular to the interferometer beam axis, hence a hole is burned in ν_2 either parallel or perpendicular to this axis. In (15b) the laser reorients some of the permanent dipoles lying along the FIR axis into the normal plane. In (15c) the laser reorients some of the

permanent dipoles that are normal to the FIR axis into that direction. The observed changes are a clear indication that the transition dipole moments of these external modes are polarized and have a fixed relationship relative to the internal molecular axes. When the permanent dipoles are rotated from the FIR axis to normal to the FIR axis as in (15b), the 71cm^{-1} mode is observed to increase. The converse is also true, as is shown in Fig. (15c). The sign and magnitude of the changes in the 71 cm^{-1} mode are consistent with a transition dipole that is along the permanent dipole axis of the molecule, hence this mode has A_1 symmetry. The higher frequency changes indicate that the polarized transition moments of the 79 cm^{-1} modes are perpendicular to the permanent dipole axis (hence B_1 or B_2 symmetry).

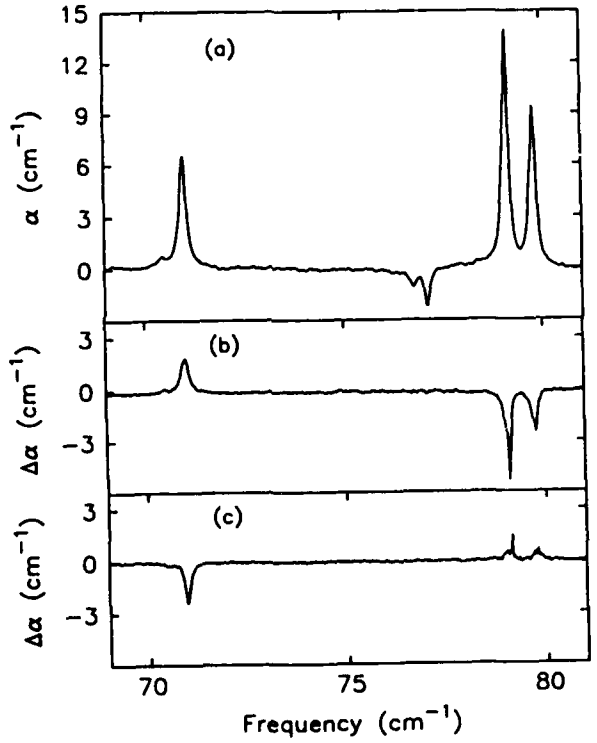

Figure 15.

In the past, one of the arguments against a local mode assignment has been that only two modes were observed in the FIR. Since now three gap modes have been resolved and since the polarized PIRSH burning results are consistent with those expected for a constrained C_{2v} molecule in a cubic site, it is reasonable to assign these modes to the three expected nondegenerate translational species: A_1, B_1, and B_2 . All evidence on the symmetry of the 71 cm^{-1} gap mode, i.e., it alone appears in combination on UV side band spectra and has been established to have its transition dipole axis parallel to the permanent

dipole axis in this work, indicates that it must transform with the A_1 representation.

One unanswered question has to do with the lifetime of these gap modes. Our high resolution FIR-IR holeburning measurements can be interpreted in either of two ways: (1) The NO_2^- gap modes are homogeneously broadened and the dephasing or T_2 time is shown in Fig. (15) or (2) These modes are inhomogeneously broadened by local strains with the frequency positions of burned homogeneous subsets for the internal bending mode and external gap modes uncorrelated. This interesting question could be settled if a tunable low intensity FIR source with a spectral width narrower than 0.1 cm^{-1} was available with which to burn persistent holes directly in these gap modes.

With the combined PIRSH burning plus FIR detection it has been possible to determine the isotope effect for the different gap modes. This measurement can be used to addressed a fundamental question in lattice dynamics theory which is now briefly described. The vibrational properties of NO_2^- in KI have long attracted interest because of the apparent conflicting signature of this substitutional defect when measured with different spectroscopic probes. One striking property is the orthogonality between direct far infrared absorption (FIR) and the Raman scattering results produced by this C_{2v} defect for impurity modes in the gap between the acoustic and optic phonon branches of the host crystal.[51,53] To account for this puzzling result Evans and Fitchen[53] noted that since parity appears to be a good quantum number the C_{2v} defect must not distort the cubic symmetry of the I^- cavity. On the other hand, parity is not conserved in the model of Rebane et al.[51] where the detailed lattice dynamical calculations of Zavt[56] are used to characterize the translational and librational motion of the molecule in the lattice. Their fit has been made with anisotropic force constants at the defect site so that the three fold degenerate translational mode associated with an isotropic defect is split. Two translational gap modes bracket a third mode which has a mixed translational and librational character. In their model it is this librational character which causes the different spectroscopic results since it makes the intermediate mode strongly Raman active and only weakly FIR active[51]. The possibility that this spectrum is mainly translational[46,47] or librational[49] in character or even that the Raman and FIR results obey the parity selection rule just as for a point defect[53] in a cubic lattice is still unresolved.

We have made the first identification of the isotope effect on the FIR gap mode spectrum by PIRSH burning and establish it as an important technique for assigning spectral lines to a particular isotopic species of NO_2^-. The substitution of ^{18}O for ^{16}O and ^{15}N for ^{14}N in NO_2^- produces gap mode frequency shifts for two of the three modes consistent with translational mode behavior. The ^{15}N for ^{14}N substitution also demonstrates that the intermediate mode for the most abundant isotopic species does have some librational character even though it does not appear in the Raman spectrum. This new level of FIR sensitivity confirms that the two spectroscopic techniques do probe orthogonal aspects of the defect dynamics.

Figure (16) shows the impurity induced spectrum obtained for a KI crystal doped with 0.1 mole % KNO_3 with 40% ^{18}O enrichment. The lines near 73, 78 and 87 cm^{-1} appear to be isotopically shifted NO_3^- modes. The broad features at 92 and 94 cm^{-1} do not show an oxygen isotope shift. PIRSH burning on the ν_2 bending mode of the (14,16,18) species with laser polarization parallel and perpendicular to the interferometer beam axis produces the FIR spectal changes shown in Fig. (16b) and (16c). Traces (16d) and (16e) show the gap mode changes produced by burning the (14,18,18) IR bending mode with the same two laser polarizations. Our investigation indicates that only spectral lines within those grouped near 71 and 79 cm^{-1} in Fig. (16) are induced by the different isotopes of the NO_2^- molecule. Without the PIRSH labelling technique, unambiguous mode identification would be extremly difficult and tedious in this mixed mode spectrum.

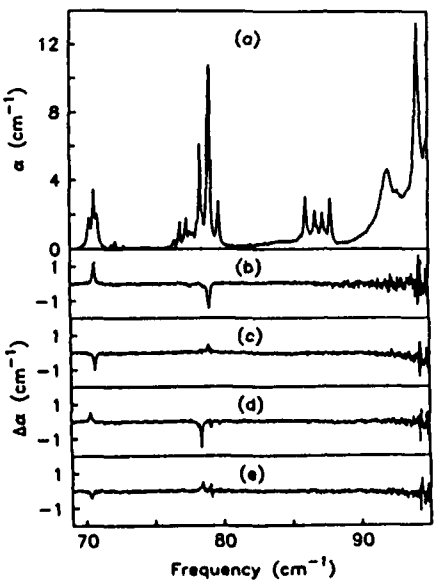

Figure 16.

3.2.4 HS in As_2S_3 glass

All persistent spectroscopic effects observed to date in glassy hosts have involved electronic excitation of the defect center, with the hole burning attributed either to photochemical modification of the defect itself, or to rearrangement of the host atoms around the defect. Because of the electronic excitation, however, the observed behavior is not necessarily representative of the glass near its ground state configuration. By using a vibrational excitation in the electronic ground state in the hole burning process, it should be possible to study behavior which is more representative of the pure, unperturbed glass. Since persistent IR spectral hole (PIRSH) burning through defect reorientation has been observed for vibrational modes of some defects in ionic crystals and van der Waals matrices[57] a search was initiated for a similar effect in glasses.

Here the first observation of PIRSH burning of an impurity vibrational mode in a glassy host is outlined. The defect-host system is the SH stretching mode in hydrogen-doped As_2S_3 glass and the results demonstrate that spectral persistence can occur in covalently bonded glasses even when the system remains in the electronic ground state. In addition to its non-electronic nature, this newly discovered PIRSH system displays unique properties which distinguish it from other systems. First, the large asymmetry of the inhomogeneous broadening mechanism for this defect allows the connection between the inhomogeneous broadening perturbation and the excited state lifetime to be studied. Second, the spectral holes become narrower as they spontaneously refill, which, to our knowledge, has not previously been observed for any system. Finally, the convenient timescale on which this refilling occurs permits it to be monitored over a much wider dynamic range than in previous work, leading to a more accurate determination of the functional form of the hole decay, which is found to be well described by a Gaussian distribution of tunnelling parameters.

Figure 17 shows the infrared absorption spectra of two samples, one doped with hydrogen, the other with deuterium. The hydrogen-doped sample displays an absorption band peaked at 2485 cm^{-1} with a full width at half maximum (FWHM) of 74 cm^{-1} at 1.5 K. Note that the band width is much larger than observed for vibrational defects in alkali halides. In the deuterated sample the absorption maximum is at 1807 cm^{-1} and the width is

51 cm^{-1}. The isotope shift by a factor of 1.375, approximately the square root of the ratio of the masses, confirms that these absorptions are vibrational in nature. The sharp line at 2323 cm^{-1} is the asymmetric stretch mode of CO_2 molecules disolved in the glass. PIRSH burning has recently been observed for this defect as well as for several others, showing that PIRSH burning is a property of the glass and does not rely strongly on the peculiarities of the specific defect.

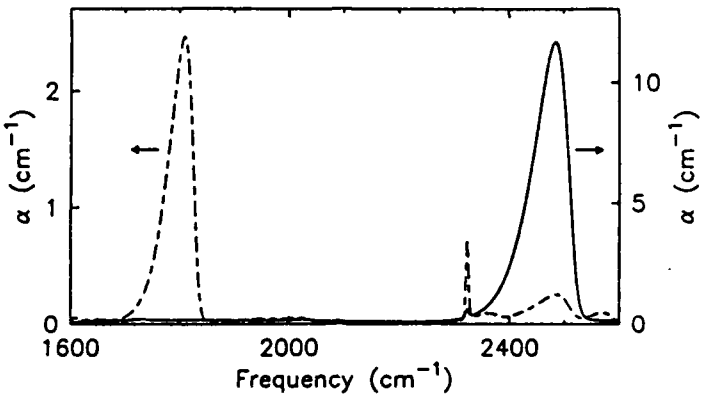

Figure 17.

Both the SH and the SD absorption bands exhibit persistent hole burning, and the behavior of the two isotopes is qualitatively similar. Holes have been burned throughout the SH band at temperatures ranging from 1.5 K up to 47 K. All holes can be erased by heating above 60 K for a few minutes.

In a typical amorphous hole burning system, spectral diffusion causes the hole width to increase with time after burning has ceased[58,59]. As can be seen in Fig. 18, however, in the As_2S_3:HS system the hole actually becomes narrower as it refills. The simplest explanation for the hole narrowing behavior is that the excited state lifetimes and dephasing rates, and hence the homogeneous widths, are not the same for all centers absorbing at a given frequency, and that those centers with the largest homogeneous linewidths return most rapidly to the original unburned configuration. The effect is seen only for relatively long burn times (several minutes) or high intensities; the broad, quickly relaxing contribution to the hole takes longer to build up than the slowly relaxing narrow contribution. Since the time evolution of the hole width is the opposite of that expected for spectral diffusion, it seems likely that spectral diffusion does not contribute significantly to the hole width. Hence the measured width in the low intensity, short burn time limit

reflects the true homogeneous width, which for Lorentzian lineshapes is half the hole width.

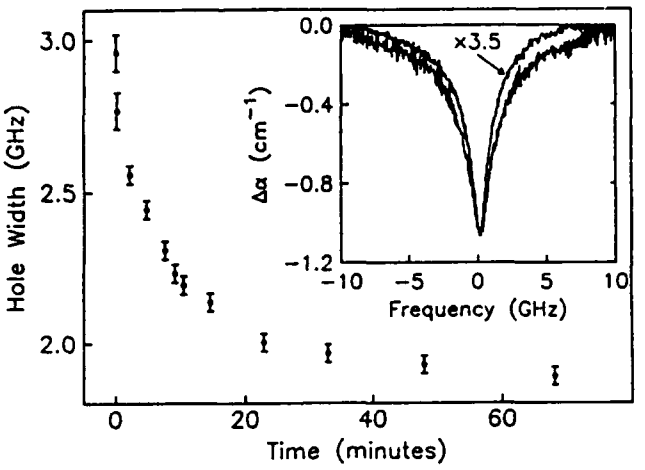

Figure 18

A striking feature of the SH and SD IR absorption bands is their highly asymmetric shape, with a sharp high frequency cutoff and long low frequency tail. This lineshape has been observed to be concentration-independent for concentrations ranging over almost three orders of magnitude, thus ruling out interactions between defects as a factor determining the lineshape. At the high frequency limit of these bands, the SH and SD stretch frequencies in As_2S_3 are only about 2 percent lower than published gas phase values for free SH and SD radicals[60-62] (2598.77 cm^{-1} and 1885.8 cm^{-1}, respectively). The absorption maxima, however, occur at a shift of about 4 percent from the gas phase values, and the low frequency tails extend to shifts of several times this amount. Since all observed SH absorption in the glass occurs at frequencies lower than for free molecules, and since there exists a sharp high frequency cutoff, it seems reasonable to interpret the asymmetric shape of the inhomogeneous band as arising from a perturbation which can only act to reduce a center's vibrational frequency. Absorption on the high frequency side of the band would then be due to relatively unperturbed centers, while strongly perturbed centers would give rise to the low frequency tail of the band.

If this picture is correct, then an SH defect's frequency shift downward from the high frequency cutoff is a measure of the host-defect coupling strength for that site. Since

both the optical dephasing rate and the excited state lifetime depend on how strongly the defect is coupled to the host, one would expect larger dephasing rates, shorter lifetimes, and hence greater hole widths, the lower the burn frequency. Figure 19 shows that this is indeed the case, and the effect is quite dramatic. Plotted is the hole width as a function of burn frequency in the short burn time limit for holes burned at 1.5 K. For burn frequencies above the absorption peak, the hole width is roughly constant, varying from 0.8 GHz at 2525 cm^{-1} to 0.9 GHz at 2497 cm^{-1}. Below this, however, the hole width increases sharply with decreasing burn frequency, growing by an order of magnitude by 2445 cm^{-1} and eventually exceeding the SDL's 0.5 cm^{-1} continuous tuning range.

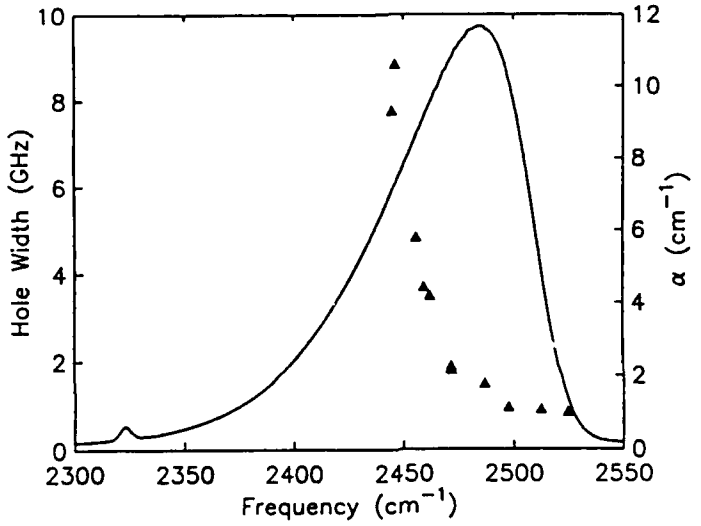

Figure 19.

In conclusion, the observation of PIRSH burning for the SH defect in As_2S_3 shows that vibrational hole burning is not restricted to ionic and van der Waals solids, but can occur in covalently bonded glasses as well. The time dependence of the spontaneous hole relaxation is well described by a Gaussian distribution of tunnelling parameters, but is strongly dependent upon the intensity used to burn the hole. The temperature dependence of the hole width suggests that the low temperature width is dominated by the excited state lifetime. The remarkable increase in hole width with decreasing burn frequency is thus a consequence of a sharp reduction of the excited state lifetime with increasing host-defect coupling.

3.2.5 Persistent hole burning in the far infrared (first attempt)

Our successful demonstration of PIRSH burning for NO_2^- in alkali halides and the observation of persistent changes in the FIR when burning in the IR leads one to ask whether persistent effects can be produced by far infrared radiation itself. The fundamental experimental problem is the absence of a tunable FIR source. Although such a source is required before such experiments can be attemped for a variety of defect-lattice systems, it has been possible to carry out such an experiment for the gap modes produced by NO_2^- with a fixed frequency source.

In our first attempt to try FIR persistent holeburning experiments we collaborated with Professor V. Jaccarino at the FIR Free Electron Laser facility at UC Santa Barbara to make use of the tunability of their source. Although it is true that this laser can be tuned to some extent it has not been possible to identify coincidences with the NO_2^- gap modes in KI. Failing there we attacked the problem at Cornell with a brute force experimental method. The approach was first to catalogue all the known fixed frequency gas laser lines in the FIR and then to measure the mode positions for different isotopic combinations of NO_2^- to identify any accidental coincidences. Since the gap modes have spectral widths of order 0.1 cm^{-1} a more accurate determination of nearby laser lines was required than was available from the published literature.

The measurement of FIR laser frequencies, good to four significant figures, required the construction of a scanning metal mesh Fabry-Perot interferometer. A side view of this instrument is shown in Fig. (20). Metal meshes with spacing to wavelength such that 99% of the radiation is reflected are stretched over parallel metal rings to form two reflectors in tandum. These free-standing mesh reflectors (A in Fig. 20), made parallel by adjustment of micrometers (B), are translated relative to each other in one micron steps by a computer-controlled stepper-motor-driven translation stage (C). Because of the high reflectivity of the mesh, FIR transmission through the pair peaks sharply whenever their separation d is a multiple of the half-wavelength (d = n 1/2 where n is an integer). This instrument has been used to measure wavelengths to a part in 10^4 and FIR laser linewidths down to 100 MHz.

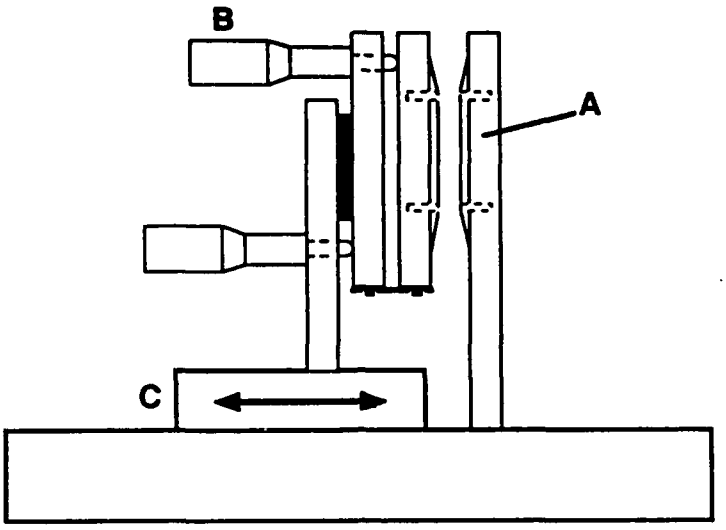

Figure 20

These results together with the isotope shifted gap modes with center frequencies identified to five significant figures are presented in Table 2. Inspection of this Table shows that a coincidence within a gap mode line width still does not occur accidentally.

In order to improve the coincidence between the fixed laser frequency and the gap mode we have prepared alloy samples. The linear dependence of the mean lattice constant on the alloy concentration is called Vegard's law. Since the gap mode frequencies also depend on the lattice constant of the host crystal, some frequency shift is to be expected in alloy crystals. We have found that this "poor man tuning" corresponds to about 0.1 cm^{-1} for every 2 mole % of KBr in KI. Similar effects have been found for other combinations. If the lattice constant of the minor component is larger than the host lattice of the major one then the gap modes move to lower frequencies upon alloying and they go in the opposite direction if the converse is true. Since the alloying broadens the modes with a width comparable to the frequency shift there is little value in using alloys above 6% so only a small shift can be realized in practice using this technique.

No persistent FIR holeburning has been observed for the three coincidences studied, see the three rows identified with a (*) in Table 2. The absence of any effect indicates that if FIR hole burning does occur the efficiency is so small that less than one photon in 10^4 converts the molecule to the new configuration. For comparison, the PIRSH efficiency for NO_2^- is 10^{-2} while the weakest optical hole burning efficiency reported for any system is 10^{-6}.

Table 2. FIR laser coincidences with gap mode frequencies in KI: NO_2^-.

DEFECT	HOST	MODE FREQUENCY (cm^{-1})	FIR GAS	CW PUMPED LINE (cm^{-1})	STATUS
$^{15}N^{16}O^{16}O^-$	KI	70.340	SO_2	70.3	70.23*
$^{14}N^{18}O^{18}O^-$	KI	70.386			
$^{14}N^{16}O^{16}O^-$	KI	70.463			
$^{14}N^{16}O^{18}O^-$	KI	70.730			
$^{15}N^{16}O^{16}O^-$	KI	70.828	CH_3NH_2	70.9	PU
$^{14}N^{16}O^{16}O^-$	KI	70.985	CH_3OD	71	U
$^{15}N^{16}O^{16}O^-$	KI	78.145	CH_3OD	78.1	U
$^{14}N^{18}O^{18}O^-$	KI	78.204			
$^{15}N^{16}O^{16}O^-$	KI	78.417			
$^{14}N^{18}O^{18}O^-$	KI	78.438			
$^{14}N^{16}O^{18}O^-$	KI	78.616			
$^{14}N^{16}O^{16}O^-$	KI	79.000	CH_3NH_2	79	78.86*
$^{14}N^{16}O^{18}O^-$	KI	79.015	CH_3NH_2	79	78.86*
$^{14}N^{16}O^{18}O^-$	KI	79.112			
$^{14}N^{16}O^{16}O^-$	KI	79.124			
$^{15}N^{16}O^{16}O^-$	KI	79.397	$C_2H_4(OH)_2$	79.4	P,U
$^{15}N^{16}O^{16}O^-$	KI	79.510	$C_2H_4(OH)_2$	79.5	P,U
$^{14}N^{16}O^{16}O^-$	KI	79.698			
$^{14}N^{16}O^{16}O^-$	KI	79.804			
$^{14}N^{16}O^{16}O^-$	KBr	97.85.	CD_3OH	97.500	G

Legend to status column:

G:	gas bought.
P:	pulsed CO_2 laser pumped line .
U:	tried, not found.

3.3 Excitations in Anharmonic Crystals and Glasses

3.3.1 Preliminaries

In the past the lattice dynamics of anharmonic crystals have been described in the same manner as for harmonic crystals. Since the atoms undergo small oscillations the important term in the potential is still harmonic. In the quasi-harmonic approximation the essential difference for the anharmonic case is that the effective harmonic potential that each atom sees is temperature dependent hence the frequencies of the plane wave phonons that are used to describe the collective vibrational modes of the system are also temperature dependent. These excitations are often referred to as renormalized phonons.

One of the most anharmonic crystals is solid ^{3}He. For such quantum systems classical lattice dynamics does not apply[63,164]; however, it is still possible to construct an effective potential energy[65] so that a semiquantitative comparison between experiment and theory is possible. A large number of experiments have been carried out on this system to test whether or not renormalized phonons provide a complete description of the vibrational excitations. The current status is that most data can be described with these excitations but yet there are some experimental results which are not consistent with the renormalized phonon model. These experiments which demonstrate the inadequacies of the current theory are mentioned here.

The early measurements of the low temperature specific heat of bcc ^{3}He showed three temperature dependent components: one which varied as T^3 and a second component which varied linearly with temperature [66-69] and at high temperatures a third component which varied exponentially with temperature[66,70]. This situation prevailed for ten years. When measurements were finally made with large crystals which had been cooled very slowly in an open geometry, the linear term was no longer observed[71] but the other two remained. These last results appeared to indicate that the source of the linear term observed by previous workers was extrinsic to solid helium. This point will be considered again later.

The extra high temperature contribution to the crystal specific heat of b.c.c. ^{3}He was determined to be of the activated form, namely,

$$C_v/R = A(f/T)^2\exp(-f/T), \qquad (13)$$

where f is the activation energy for a particular molar volume. This form for the excess specific heat contribution does not uniquely identify the mechanism since it is consistent with an Einstein oscillator term (A = 3), a two level Schottky anomaly (A = g_1/g_0) where g_1 and g_0 are the degeneracy of the excited state and the ground state, respectively, vacancy formation (A = 1), vacancies and interstitials individually (A = 4), or vacancy-interstitial pairs(A = 3.5)[67,71]. The original data was fit with A =2 but the most recent and most accurate heat capacity measurements show that the contribution is best fit with A ≈ 1, that A is temperature dependent, and that $f \sim \Theta_D^2$, where Θ_D is the Debye temperature for a particular molar volume at 0 K [71]. The idea that this effect is associated with vacancy formation (A = 1) has been pursued by a number of workers [71-73].

A direct determination of an activated volume change in ^{3}He has been obtained from measurements of the temperature dependence of the x-ray lattice parameter in a constant volume cell[74, 75]. The thermal vacancy concentration is equal to the change in the macroscopic volume of a cell minus the microscopic x-ray volume. With this number determined, it has been shown that the localized vacancy assumption gives too large a specific heat contribution to be consistent with the measured data. Together the specific heat and x-ray data demonstrate that nonlocalized vacancies may occur.

Glasses also show anomalous temperature dependencies in the thermodynamic properties. In addition, as a function of temperature the low temperature specific heat of glasses shows a universal form[76,77]. At low temperatures the specific heat varies linearly with temperature while for higher temperatures the T^3 dependence is observed but the coefficient of this Debye specific heat term is 10% to 100% larger than the value calculated from the measured sound velocities in the same material[77,78].

An early explanation of the linear term made use of tunneling of atoms or groups of atoms in the disordered solid. An ad hoc assumption that the density of tunneling states was a constant independent of energy was required to explain the observed temperature dependence[79,80]. Although the tunneling model is still used to describe the low temperature experimental data, during the past 18 years a convincing argument which produces both of the characteristic thermal properties, namely the linear term and the enhanced coefficient of the Debye term, has not been forthcoming.

3.3.2 Anharmonic localized modes in crystals and glasses

During this grant period the PI in collaboration with Professor S. Takeno from Japan have come up with a new model to describe the dynamics of anharmonic crystals and glasses. The proposal was described in a series of four concise and fairly mathematical papers[81-84]. Here the model is described in a qualitative manner to bring out the key features which can account for some of the unexplained experimental data described in the previous section.

To visualize how localized modes can appear in a perfect but anharmonic lattice the one dimensional harmonic lattice is considered first. The normal modes are described by an orthogonal set of plane homogeneous waves which are spread through a band of frequencies. An excitation localized at a particular site can be constructed from a linear superposition of these normal modes and this localized wave packet centered around a particular frequency in the band moves through the crystal in the usual way.

For a one dimensional anharmonic lattice in the limit of small oscillations the plane wave spectrum looks the same as for the harmonic case. What happens if one constructs a wave packet to represent a localized vibration in the chain? To be specific let us assume that the anharmonicity is quartic with a positive coefficient. As the wave packet is constructed the amplitude of the atom increases and since the potential is not harmonic so does its frequency of vibration. Now as one localizes an excitation more and more around a particular atom the amplitude of vibration gets larger and the center frequency moves up through the band of allowed frequencies until it pops out of the top of the spectrum. Given sufficient anharmonicity the end result is a true localized mode centered at the atom in question. The anharmonic system has evolved in such a way that both homogeneous and inhomogeneous waves exist.

The eigenvector of the highest frequency mode for three specific cases are shown in Fig. (21). Case (c) depicts the highest frequency (ω_m) plane wave mode of the harmonic linear chain. With increasing anharmonicity a localized solution exists, (b), which is separated off from the plane wave spectrum so that there are now only N-1 plane wave modes and one localized mode with $\omega_l > \omega_m$. For this case there are roughly N_d atoms involved in the localized vibration and since $N_d << N$ the amplitude of each atom in this

mode is much larger than for the plane wave case. In the high frequency limit, $\omega_{l'} >> \omega_m$, the local mode eigenvector takes on the particularly simple form shown in case (a) with the excitation completely localized on the central atom and its two neighbors.

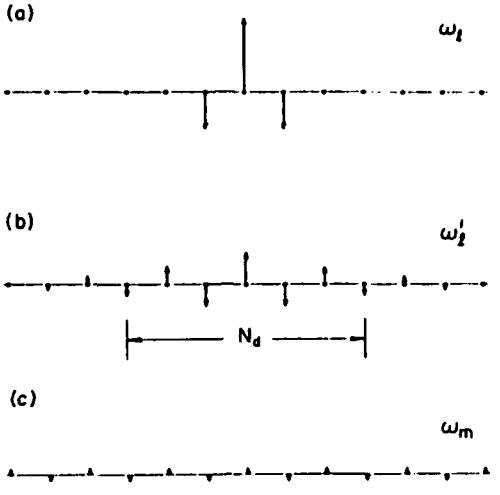

Figure 21

A schematic representation of the frequencies associated with the plane wave spectrum located between 0 and ω_m and the anharmonic localized mode at $\omega_{l'}$ is shown in Fig. (22b). The relative frequency of the localized mode to ω_m depends on the relative magnitudes of the anharmonic and harmonic potential terms. Also shown in the picture is a dashed line which represents the position of the local mode third harmonic. In principle, the anharmonic potential produces a response at this frequency, but because it is so much larger than the plane wave and the local mode frequencie, it is assumed that the lattice cannot respond and so it is ignored in the dynamical analysis. This assumption is usually referred to as the rotating wave approximation.

Somewhat harder to visualize is the resonant mode which occurs in the case of the soft anharmonic lattice. Once again a localized excitation results, but now at low frequencies the central atom vibrates against the rest of the crystal lattice. The characteristic frequencies in this problem are shown in Fig. (22a). The resonant mode is far down in the acoustic spectrum so $\omega_r << \omega_m$. The corresponding eigenvector is shown on the right. Note that for this soft potential case a response at the third harmonic is possible since it occurs at an energy in the plane wave spectrum. This additional channel shortens the lifetime of the resonant mode and makes it less well defined than for the local mode.

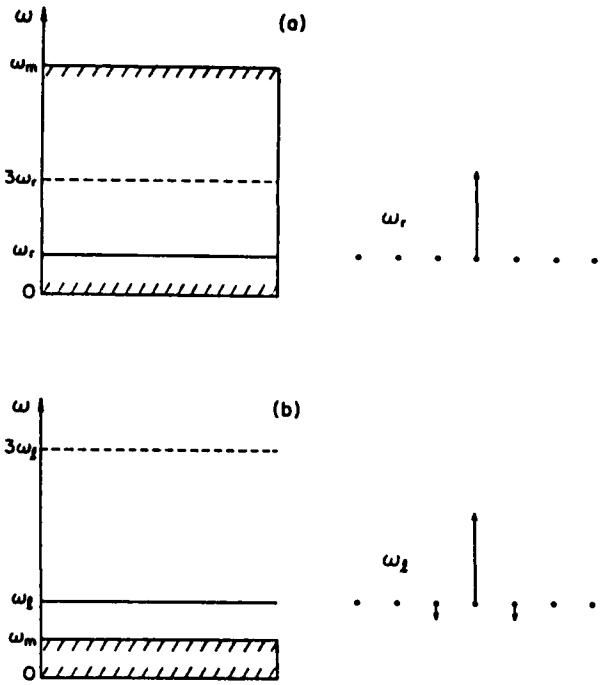

Figure 22.

With the form of the solutions identified for the two kinds of potentials the next step is to introduce temperature into the problem. Consider the dynamics of a quantum mechanical one dimensional harmonic lattice of N atoms in thermal equilibrium with a heat reservoir. At absolute zero temperature each mode in the bounded plane wave spectrum has a zero point energy of $\hbar\omega/2$. Because all atoms are involved in each mode the root mean square amplitude of a given atom is $N^{-1/2}$ times the value it would have if only this one atom was involved in this particular mode. At low temperature the lowest energy modes of the system within kT of the zero point states become thermally excited giving rise to phonons. Most of the higher frequency modes remain in their zero point ground states but in any event all excitations are still described by plane waves..

Now consider what happens in the case of the anharmonic crystal. At absolute zero temperature the plane wave description applies just as for the harmonic case above. However, the situation is quite different at finite temperature since as shown above both homogeneous and inhomogeneous wave solutions can occur. Given kT of energy per atom the system can either distribute it over the plane wave spectrum producing phonons in the usual way, or use some of the energy to create high frequency localized modes in their zero point motion ground states (for the case of positive quartic anharmonicity) or low frequency resonant modes (for the case of negative quartic anharmonicity). These localized

excitations will be referred to as "anons" in the rest of the discussion. Since it takes energy to create an anon in its zero point state this event would be extremely unlikely if only energy was involved. But the creation of a localized defect in a perfect lattice also produces a large configurational or entropy of mixing term since the defect can appear at any one of the N lattice sites, hence to determine their existence it is important to keep track of the free energy of the system. For the one dimensional lattice considered here the entropy term is still not large enough to make localized defects occur.

Only in three dimensions does the entropy become large enough to change the sign of the free energy of the lattice so that localized states automatically appear at finite temperature. The argument is similar to that used to account for vacancies in crystals however the energy scale is much smaller now since the atom is not required to move out of a given lattice site, instead the atom remains at its equilibrium position and a localized strain field accompanies the creation of each anon. The number of anons in the crystal at any temperature T obeys an activation law. We have proposed that the activation term found in the experimental specific heat of solid ^{3}He may stem from the production of these anon modes[82].

So far the discussion has been limited to stationary anons in crystalline lattices. Because all lattice sites are equivalent it is expected that these modes could translate. How easily they move is still an unanswered question. The answer must depend to some extent on the incommensurability of the length scale of the shape function of the anon with respect to the lattice spacing.

If anons do not translate but in fact diffuse through the lattice, then this motion produces a contribution to the specific heat which is linear in temperature[84,85]. However, because of the activation energy required to produce these modes, the number density is too small to detect at low temperatures in ordinary dielectric crystals.

The situation is very different in glasses since disorder is frozen in upon cooling through the glass transition temperature. If it is assumed that the structural disorder makes local volume fluctuations in the solid which are compatible with the requirements of the anon configurations, then the maximum number of these modes become available at all temperatures below the glass transition temperature. In contrast with the anharmonic single

crystal where, because of the activation energy associated with the localized configurations, the low temperature modes are essentially all phonons, the disordered solid contains both phonons and anons. The phonons give a T^3 contribution to the specific heat of glass and the diffusing anons, a linear term.

The anons also explain the fact that the T^3 contribution is enhanced over what is calculated from the velocity of sound measurements. Assume that the anons are associated with resonant modes. In the limit that the density of resonant modes is small, the total low temperature specific heat of the disordered solid is assumed to consist of a sum of linearly independent contributions in analogy with the defect resonant mode case in crystals so

$$C_V(T) = (n - n_a)c_D + n_a c_{ad} + n_a c_{av} \qquad (14)$$

where the first and last terms describe the contribution from Debye and stationary resonant mode vibrational degrees of freedom which so far have been ignored. Note that since the the resonant mode is stationary it does not contribute in a propagating pulse experiment such as is carried out in a sound velocity measurement. For $n >> n_a$ Eq. (14) simplifies to

$$C_V(T) \approx nc_D + n_a c_{ad} + n_a c_{av} \qquad (15)$$

To estimate $n_a c_{av}$ in Eq. (15) requires knowledge of the density of vibrational states below the resonant mode center frequency. Although this quantity is not yet available for anharmonic resonant modes, the eigenvalue equation for the anharmonic mode is similar to that obtained for a harmonic resonant mode produced by a force constant defect. The mean square amplitude of the atom located at site 0 versus frequency is shown for the force constant defect in Fig. (23). If this analogy carries over to the calculation of the low frequency density of states, which we now assume, then for the limit where $\omega < \omega_r$, the extra low frequency contribution to the vibrational density of states varies as ω^2 just as for the plane wave spectrum. Since the form is quadratic in frequency, this vibrational component will provide a T^3 contribution to the specific heat. The trade off between the increased density of states at frequencies below the resonance and the relatively small number density of resonant mode centers is such that a significant contribution to the T^3 specific heat results. We find that $C_{av}/C_D = 0.25$, a constant in the low temperature limit.

The anon model predicts two interrelated signatures in the low temperature specific heat of glasses: a T^3 term which stems from an enhanced density of vibrational modes in

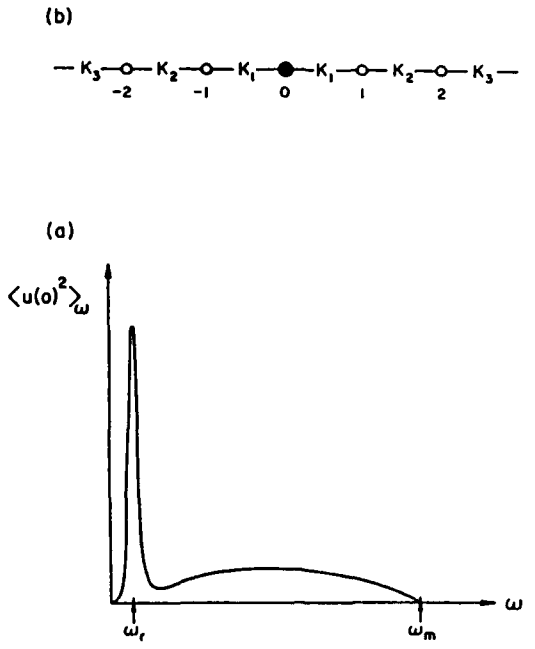

Figure 23.

the neighborhood of ω_r and a linear term which appears because these resonant mode centers can diffuse. Both of these features have been found to be universal properties of glasses.

Because of diffusion the anon center of mass motion cannot contribute to the propagation of an energy pulse the way a plane wave mode can. In addition, its localized vibrational degree of freedom corresponds to a standing wave so it cannot contribute either. These characteristics are consistent with the idea that the anon contribution will remain partially hidden in any experiment which probes the propagation of waves through the solid such as a velocity of sound measurement.

4. PUBLICATIONS (1986 -1989)

(Note: A ® in front of the publication indicates that the work was supported by ARO.)

Papers

® "Persistent Infrared Hole-burning Spectroscopy of Matrix-isolated CN^- Molecules," R. C. Spitzer, W. P. Ambrose and A. J. Sievers, Optics Letters **11**, 428 (1986).

"Surface Reconstruction Induced Changes in Free Carrier Scattering from the W(100) Surface: An Infrared Surface Electromagnetic Wave Study," D. M. Riffe, L. M. Hanssen and A. J. Sievers, Physical Review B **34**, 692 (1986).

"Infrared Observation of Adsorbate Induced Changes in Free Carrier Surface Scattering," D. M. Riffe, L. M. Hanssen and A. J. Sievers, Surface Science **176**, 679 (1986).

® "Intensity-dependent Cyclotron Resonance in a GaAs/GaAlAs Two-dimensional Electron Gas," G. A. Rodriguez, R. M. Hart, A. J. Sievers, F. Keilmann, Z. Schlesinger, S. Wright, and W. I. Wang, Applied Physics Letters **49**, 458 (1986).

"Proton Tunneling with meV Energies at the Be:H Acceptor Complex in Silicon," K. Muro and A. J. Sievers, Physical Review Letters **57**, 897 (1986).

" Reply to "Comment on 'Observation of an index-of-refraction-induced change in the Drude parameters of Ag films', " H. Gugger, M. Jurich, J. D. Swalen, and A. J. Sievers, Phys. Rev. B **34**, 1322 (1986).

"Observation of an Energy and Temperature Dependent Carrier Mass for Mixed Valence $CePd_3$," B. C. Webb, A. J. Sievers, and T. Mihalisin, Physical Review Letters **57**, 1951-1954 (1986).

" Infrared Surface Wave Interferometry on W(100)," L. M. Hanssen, D. M. Riffe, and A. J. Sievers, Optics Letters **11**, 782 (1986).

® " Observation of Persistent IR Hole Burning in the Vibrational Spectrum of CN- in KBr," R. C. Spitzer, W. P. Ambrose, and A. J. Sievers, Physical Review B **34**, 7307 (1986).

" Incoherent Saturation Study of the Selenium Donor in AlSb," R. E. Peale, K. Muro, J. T. McWhirter, and A. J. Sievers, Solid State Communications **60**, 753-755 (1986).

"Hemispherical Emissivity of V, Nb, Ta, Mo, and W from 300 to 1000 K," S. X. Cheng, P. Cebe, L. M. Hanssen, D. M. Riffe, and A. J. Sievers, Journal of the Optical Society of America B **4**, 351 (1987).

" Observation of Tunneling at Deep Level Acceptor Complexes in Silicon," K. Muro and A. J. Sievers, Proceedings of the 18th International Conference on the Physics of Semiconductors, O. Engström, ed. (World Scientific, 1987) vol. 2, p. 891.

® "Measurement of the Superconducting Energy Gap in La-Ba-Cu Oxide and La-Sr-Cu Oxide," P. E. Sulewski, A. J. Sievers, S. E. Russek, H. D. Hallen, D. K. Lathrop, and R. A. Buhrman, Physical Review B **35**, 5330 (1987).

® "Far Infrared Measurements of $\alpha^2(\omega)F(\omega)$ in Superconducting $La_{1.84}Sr_{0.16}CuO_{4-y}$," P. E. Sulewski, A. J. Sievers, R. A. Buhrman, J. M. Tarascon, L. H. Greene, and W. A. Curtin, Physical Review B **35**, 8829 (1987).

® "Persistent Spectral Hole Burning in Solids Using Lead-Salt Lasers," A. J. Sievers, The Laser Analytics Letter **8**, 1 (1987).

® "Free Carrier Relaxation Dynamics in the Normal State of Sintered $YBa_2Cu_3O_{7-y}$," P. E. Sulewski, T. W. Noh, J. T. McWhirter, A. J. Sievers, S. E. Russek, R. A. Buhrman, C. S. Jee, J. E. Crow, R. E. Salomon, and G. Myer, Physical Review B **36**, 2357 (1987).

"IR Spectral Hole Burning of S-H Deep Donors in a Si:Ge Crystal," S. P. Love, K. Muro, R. E. Peale, and A. J. Sievers, Physical Review B **36**, 2590 (1987).

® "Far Infrared Composite Medium Study of Sintered La_2NiO_4 and $La_{1.85}Sr_{0.15}CuO_{4-y}$," P. E. Sulewski, T. W. Noh, J. T. McWhirter, A. J. Sievers, Physical Review B **36**, 5735 (1987).

® "Comparison of the Electrodynamic Properties of Sintered $YBa_2Cu_3O_{7-y}$ and $La_{1.85}Sr_{0.15}CuO_{4-y}$," T. W. Noh, P. E. Sulewski, and A. J. Sievers, Physical Review B **36**, 8866 (1987).

® "Vibrational Relaxation Dynamics of Matrix-Isolated BH2D2-," D. M. Kammen, T. R. Gosnell, R. W. Tkach, and A. J. Sievers, Journal of Chemical Physics **87**, 4371 (1987).

® "Persistent Infrared Spectral Hole-Burning for Impurity Vibrational Modes in Solids," A. J. Sievers and W. E. Moerner, in Persistent Spectral Hole-Burning: Science and Applications, W. E. Moerner, Editor (Springer-Verlag Publishing Co., New York, 1988) Chapter 6.

"Zeeman Splitting of Double-Donor Spin-Triplet Levels in Silicon," R. E. Peale, K. Muro, A. J. Sievers and F. S. Ham, Phys. Rev. B **37**, 10829 (1988).

® "Far Infrared Measurements on Single Crystals, Films, and Bulk Sintered High

Temperature Superconductors," T. W. Noh, P. E. Sulewski, S. G. Kaplan, A. J. Sievers, D. K. Lanthrop and R. A. Buhrman, Mat. Res. Soc. Symp. Proc. **99**, 435 (1988).

® "Microwave Superconductivity for Particle Accelerators - How the High Tc Superconductors Measure Up", H. Padamsee, K. Green, J. Gruschus, J. Kirchgessner, D. Moffat, D. L. Rubin, J. Sears, Q. S. Shu, R. Buhrman, D. Lathrop, T. W. Noh, S. Russek, and A. J. Sievers, Conference on Superconductivity and Applications, Institute on Superconductivity, SUNY Buffalo, April 18-20, 1988.

® "Far Infrared Measurements on Single Crystals, Films, and Bulk Sintered High Temperature Superconductors", T. W. Noh, P. E. Sulewski, S. G. Kaplan, A. J. Sievers, D. K. Lanthrop and R. A. Buhrman, Mat. Res. Soc. Symp. Proc. **99**, 435 (1988).

® "Optical Pumping of Vibrational Overtones in KI:CN- Infrared Lasers", T. R. Gosnell, A. J. Sievers, and C. R. Pollock, Optics Letters **13**, 631 (1988).

® "Intrinsic Localized Modes in Anharmonic Crystals", A. J. Sievers and S. Takeno, Physical Review Letters **61**, 970 (1988).

® "Anharmonic Resonant Modes in Perfect Crystals", S. Takeno and A. J. Sievers, Solid State Communications, **67**, 1023 (1988).

® "Persistent Changes in the FIR Spectrum of KI:NO_2^- Produced by IR Vibrational Hole Burning", W. P. Ambrose and A. J. Sievers, Chemical Physics Letters **147**, 608 (1988).

® "Optical Reflectivity Studies of Polycrystalline LaBaCuO and LaSrCuO", S. G. Kaplan, T. W. Noh, P. E. Sulewski, H. Xia, and A. J. Sievers, Physical Review B **38**, 5006 (1988).

® " The Far Infrared Absorptivity of UPt_3", P. E. Sulewski, A. J. Sievers, M. B. Maple, M. S. Torikachvili, J. L. Smith and Z. Fisk, Physical Review B **38**, 5338 (1988).

® "Isotope-shift measurement of the NO_2^- gap mode spectrum in KI with persistent IR spectral holes", W. P. Ambrose and A. J. Sievers, Physical Review B **38**, 10170 (1988).

® "Intrinsic Localized Vibrational Modes in Anharmonic Crystals", S. Takeno, K. Kisoda and A. J. Sievers, Progess of Theoretical Physics, Supplement **94**, 242 (1988).

® "Persistent Infrared Spectral Hole Burning of the SH Vibrational Mode in Hydrogenated As_2S_3 Glass", S. P. Love and A. J. Sievers, Chemical Physics Letters **153**,379 (1988).

® "Determination of the Orientation of NO_2^- in KI by Persistent IR Spectral Hole Burning", W. P. Ambrose and A. J. Sievers, physica status solidi (b) **151**, (1989).

"Zeeman Splitting of Double-Donor Spin-Triplet Levels in Silicon", R. E. Peale, R. M. Hart, A. J. Sievers and F. S. Ham, Proceedings of the Third International Conference on Shallow Impurities in Semiconductors, Linköping, Sweden, August (1989).

® "Observation of a Far-Infrared Sphere Resonance in Superconducting $La_{2-x}Sr_xCuO_{4-y}$ Particles", T. W. Noh, S. G. Kaplan and A. J. Sievers, Physical Review Letters **62**, 599 (1989).

® "Anharmonic Resonant Modes and the Low Temperature Specific Heat of Glasses", A. J. Sievers and S. Takeno, Phys. Rev. B (1989).

"Infrared Reflection-Absorption Spectroscopy of W(100)-H at 100 K", D. M. Riffe and A. J. Sievers, Surface Science (1989).

® "Far Infrared Difference Band Absorption in Pottassium Iodide", S. P. Love, W. P. Ambrose and A. J. Sievers, Phys. Rev. B (1989).

Published Talks

® "Persistent Spectral Hole Burning in the Vibrational Modes of KBr:NO_2^-", W. P. Ambrose and A. J. Sievers, Bull. Amer. Phys. Soc. **31**, 278 (1986).

® "Exploring Persistent Effects in the Vibrational Spectrum of KBr:CN^-:Na^+ with Tunable Diode Lasers", R. C. Spitzer, W. P. Ambrose and A. J. Sievers, Bull. Amer. Phys. Soc. **31**, 278 (1986).

® "Spectroscopy of Persistent Spectral holes and Antiholes in a Vibrational Absorption Band of Matrix isolated Molecules Using Stark Modulation Techniques", T. R. Gosnell, R. W. Tkach and A. J. Sievers, Bull. Amer. Phys. Soc. **31**, 278 (1986).

® "Exploring V-V Transfer between CN^- Molecules in Alkali Halides", R. C. Spitzer and A. J. Sievers, Bull. Amer. Phys. Soc. **32**, 894 (1987).

® "Persistent Changes in the Phonon-Gap Mode Spectrum of NO_2^- in KI Induced by IR Hole Burning", W. P. Ambrose and A. J. Sievers, Bull. Amer. Phys. Soc. **32**, 894 (1987).

® "Vibrational Emission from Nonresonantly Excited CN^- Molecules in Alkali Halide Crystals", J. T. McWhirter, W. P. Ambrose and A. J. Sievers, Bull. Amer. Phys. Soc. **32**, 894 (1987).

® "Far-IR Intensity dependence of the Cyclotron resonance of a 2-DEG Electron Gas," G.

A. Rodriguez, R. M. Hart, A. J. Sievers, and Z. Schlesinger, J. Optical Society of America A **4**, 28 (1987).

"Infrared Spectral Hole Burning of Defects in Elemental Semiconductors," S. P. Love, K. Muro, R. E. Peale, and A. J. Sievers, J. Optical Society of America A **4**, 48 (1987).

"Zeeman Spectroscopy on Deep Double Donors in Si: the Solid State Analogue of the Helium Atom," R. E. Peale, K. Muro, A. J. Sievers, and F. S. Ham, J. Optical Society of America A **4**, 65 (1987).

® "Nonresonant Satellite Holes Produced by Persistent Spectral Hole Burning in KCl:NO_2^-," W. P. Ambrose and A. J. Sievers, J. Optical Society of America A **4**, 73 (1987).

® "Dynamics of UV-induced Vibrational Fluorescence of the CN^- Ion in Alkali Halides," J. T. McWhirter, W. P. Ambrose and A. J. Sievers, J. Optical Society of America A **4**, 73 (1987).

® "Microwave Superconductivity for Particle Accelerators - How the High Tc Superconductors Measure Up," H. Padamsee, K. Green, J. Gruschus, J. Kirchgessner, D. Moffat, D. L. Rubin, J. Sears, Q. S. Shu, R. Buhrman, D. Lathrop, T. W. Noh, S. Russek, and A. J. Sievers, Conference on Superconductivity and Applications, Institute on Superconductivity, SUNY Buffalo, April 18-20, 1988.

® "Influence of Persistent IR Hole Burning on Far Infrared Gap Modes," W. P. Ambrose and A. J. Sievers, Bull. Amer.Phys. Soc. **33**, 775 (1988).

® "Persistent IR Spectral Hole Burning in Hydrogen-doped As_2S_3 Glass," S. P. Love and A. J. Sievers, Bull. Amer.Phys. Soc. **33**, 784 (1988).

® "Vibrational Stark Effect for Matrix Isolated CN^- Molecules," R. C. Spitzer, A. J. Sievers, and R. H. Silsbee, Bull. Amer.Phys. Soc. **33**, 776 (1988).

® "Optical Response from 1 meV to 3.8 eV of Single-Crystal $YBa_2Cu_3O_{7-y}$," P. E. Sulewski, T. W. Noh, and A. J. Sievers, Bull. Amer.Phys. Soc. **33**, 416(1988).

® "Far Infrared Reflectivity Measurements on Single-Crystal $YBa_2Cu_3O_{7-y}$," T. W. Noh, P. E. Sulewski, and A. J. Sievers, Bull. Amer.Phys. Soc. **33**, 451(1988).

® American Physical Society Frank Isakson Prize Lecture: "Far Infrared Electrodynamics of Oxide Superconductors", A. J. Sievers, Bull. Amer. Phys. Soc. **33**, 507 (1988).

® invited paper: "Far Infrared properties of oxide superconductors", A. J. Sievers, Optical

Society of America, 1988 Annual Meeting

® invited paper: "Exploring the low lying excitation spectra of high T_c superconductors", A. J. Sievers, Thirteenth International Conference on Infrared and Millimeter Waves, The International Society for Optical Engineering, 1039 (1988).

® "KI:NO_2^- Gap Mode Assignments by Persistent IR Hole Burning and FIR Isotope Shifts", W.P. Ambrose and A.J. Sievers, Bull. Amer. Phys. Soc. March (1989).

® "Persistent IR Spectral Hole Burning of Impurity Vibrational Modes in Chalcogenide Glasses", S. P. Love and A. J. Sievers, Bull. Amer. Phys. Soc. March (1989).

® "Diffuse Infrared Reflectivity Study of Sintered $YBa_2Cu_3O_{7-y}$ ", A. Rosenberg, A. S. Barker, T. W. Noh and A.J. Sievers, Bull. Amer. Phys. Soc. March (1989).

® "Magnetic Field Dependence of the Far Infrared Nonlinear Susceptibility of Free Carriers in n-InP", R. M. Hart, G. A. Rodriguez, S. A. FitzGerald, A. J. Sievers, Bull. Amer. Phys. Soc. March (1989).

® invited paper: "Observation of a Far-Infrared Sphere Resonance in Superconducting $La_{2-x}Sr_xCuO_{4-y}$ Particles", T. W. Noh, Bull. Amer. Phys. Soc. March (1989).

® invited paper: "Energy Dependent Scattering in Heavy Fermion Compounds", P. E. Sulewski, Bull. Amer. Phys. Soc. March (1989).

® "Far Infrared Transmission Measurements of $YBa_2Cu_3O_{7-y}$ Thin Films", S. G. Kaplan, T. W. Noh, A. J. Sievers, S. E. Russek, and R. A. Buhrman, Bull. Amer. Phys. Soc. March (1989).

® "IR Emission from UV Irradiated Alkali Halide Crystals Containing Point Defects", J. T. McWhirter and A. J. Sievers, Bull. Amer. Phys. Soc. March (1989).

® "Hot Carrier 2D Cyclotron Resonance Near the Intersubband Energy", G. A. Rodriguez, R. M. Hart, Z. Schlesinger and A. J. Sievers, Bull. Amer. Phys. Soc. March (1989).

Theses

® "Dielectric properties of the Exited State Off-Center Configuration of Silver Doped KI", S. B. Hearon, M.S. Thesis, Cornell University (1986).

® "A Solid State Vibrational Laser", T. R. Gosnell, Ph. D. Thesis, Cornell University (1986).

"Infrared Dynamical Conductivity of the Valance-Fluctuating Alloys of $CePd_3$, B. C. Webb, Ph. D. thesis, Cornell University (1986).

® "IR Vibrational Fluorescence and Persistent Hole Burning from CN^- Molecules in Alkali Halides", R. C. Spitzer, Ph. D. Thesis, Cornell University (1988).

® "Electrodynamics of Heavy Fermion Compounds and High T_c Superconductors", P. E. Sulewski, Ph. D. Thesis, Cornell University (1988).

5. REFERENCES

1. J. G. Bednorz and K. A. Müller, Z. Phys. B 64, 189 (1986); M. K. Wu, et al., Phys. Rev. Lett. 58, 908 (1987).
2. G. Brändli and A. J. Sievers, Phys. Rev. B 5, 3550 (1972).
3. D. C. Mattis and J. Bardeen, Phys. Rev. 111, 412 (1987).
4. M. Tinkham, in Far-Infrared Properties of Solids, ed. S.S. Mitra and S. Nudelman, (New York: Plenum Press, 1970), p. 223.
5. T. Holstein, Phys. Rev. 96, 535 (1954).
6. R. R. Joyce and P. L. Richards, Phys. Rev. Lett. 24, 1007 (1970).
7. P. B. Allen, Phys Rev. B 3, 305 (1971).
8. H. Scher, Phys. Rev. B 3, 3551 (1971).
9. G. Brandli, Phys. Rev. Lett. 28, 159 (1972).
10. P. E. Sulewski, et al., Phys. Rev. B 36, 2357 (1987).
11. D. A. Bonn, et al., Phys. Rev. Lett. 58, 2249 (1987).
12. G. A. Thomas, H. K. Ng, et al., Phys. Rev. B 35, 846 (1987).
13. L. Genzel, et al., Sol. St. Commun. 63, 643 (1987).
14. F. E. Pinkerton, et al., Phys. Rev. B 30, 3068 (1984).
15. J. M. Bassat, P. Odier, and F. Gervais, Phys. Rev. B 35, 7126 (1987).
16. P. E. Sulewski, et al., Phys. Rev. B 36, 5735 (1987).
17. T. W. Noh, P. E. Sulewski, and A. J. Sievers, Phys. Rev. B 36, 8866 (1987).
18. K. Kamaras et al., Phys. Rev. Lett. 59, 919 (1987).
19. J. Orenstein, et al., Phys. Rev. B 36, 729 (1987); S. L. Herr, et al. Phys. Rev. B 36, 733 (1987); J. Orenstein et al., Phys. Rev. B 36, 8892 (1987); S. Etemad, et al., Phys. Rev. B 37, 3396 (1988).
20. C. M. Varma, S. Schmitt-Rink, and E. Abrahams, Solid State Commun. 62, 681 (1987); M. J. Rice and Y. R. Wang, Phys. Rev. B 36, 8794 (1987); W. Weber, Bull. Am. Phys. Soc. 33, 459 (1988).
21. Z. Schlesinger, et al., Phy. Rev. Lett. 59, 1958 (1987); G. A. Thomas et al., Jpn. J. Appl. Phys. 26, suppl. 26-3 (1987).

22. S. Tajima et al., Mod. Phys. Lett. B 1, 353 (1988).

23. P. E. Sulewski, et al., Bull. Am. Phys. Soc. 33, 417 (1988).

24. S. G. Kaplan, et al., Phys. Rev. B38, 5006 (1988).

25. J. B. Torrance, et al., Phys. Rev. Lett. 60, 542 (1988).

26. J. Orenstein and D. H. Rapkine, Phys. Rev. Lett. 60, 968 (1988).

27. T. W. Noh, et al., Mat. Res. Soc. Symp. Proc. 99, 435 (1988).

28. T. Timusk, et al., Phys. Rev. B 38, 6683 (1988).

29. N. P. Ong, et al., Phys. Rev. B 35, 8807 (1987).

30. S. von Molnar, et al., Phys. Rev. B 37, 3762 (1988).

31. Z. Schlesinger et al., Phys. Rev. Lett. 59, 1958 (1987).

32. G. A. Thomas et al., Phys. Rev. Lett. 61, 1313 (1988).

33. D. B. Tanner et al., Physica C 153-155, (1988).

34. G. A. Thomas et al., Phys. Rev. B 36, 736 (1987); Z. Schlesinger et al., Phys. Rev. B 36, 5275 (1987); P. E. Sulewski et al., Phys. Rev. B 36, 5735 (1987); M. S. Sherwin et al., Phys. Rev. B 37, 1587 (1988).

35. P. E. Sulewski et al., Phys. Rev. B 35, 5330 (1987); U. Walter et al., Phys. Rev. B 35, 5327 (1987); D. A. Bonn, Solid State Comm. 62, 383 (1987); K. Nagasaka et al., Jpn. J. Appl. Phys. 26, L481 (1987); D. A. Bonn, Phys. Rev. B 35, 8843 (1987);

36. R. Ruppin and R. Englman, Rep. Progr. Phys. 33, 149 (1970); L. Genzel and T. P. Martin, Surf. Sci. 34, 33 (1973).

37. T. W. Noh, S. G. Kaplan, and A. J. Sievers, Phys. Rev. Lett. **62**, 599 (1989).

38. M. Tinkham, in Superconductivity, (New York, Gordon and Breach, 1965), p.22.

39. W. E. Moerner, J. Mol. Electronics 1, 55 (1985).

40. M. Dubs, Hs. H. Günthard, Chem. Phys. Letters 64, 105-107 (1979); M. Dubs, Hs. H. Günthard, J. Mol. Structure 60, 311 (1980) and M. Dubs, L. Ermanni, Hs. H. Günthard, J. Mol. Spectry. 91, 458 (1982).

41. W. E. Moerner, A. J. Sievers, R. H. Silsbee, A. R. Chraplyvy, D. K. Lambert, Phys. Rev. Lett. 49, 398 (1982); W. E. Moerner, A. R. Chraplyvy, A. J. Sievers, R. H. Silsbee, Phys. Rev. B 28, 7244-7259 (1983); T. R. Gosnell, A.

J. Sievers, R. H. Silsbee, Phys. Rev. Lett. 52, 303 (1984) and R. C. Spitzer, W.P. Ambrose, A. J. Sievers, Opt. Lett. 11, 428 (1986).

42. R. C. Spitzer, W.P. Ambrose, A. J. Sievers, Phys. Rev. B 34, 7307 (1986).
43. W. P. Ambrose and A. J. Sievers, Chemical Physics Letters 147, 608 (1988).
44. S. P. Love, K. Muro, R. E. Peale, and A. J. Sievers, Physical Review B 36, 2590 (1987).
45. S. P. Love and A. J. Sievers, Chemical Physics Letters 153,379 (1988).
46. A.J. Sievers and C.D. Lytle, Physics Lett. 14 (1965) 271.
47. K.F. Renk, Phys Lett. 14 (1965) 281.
48. A. S. Barker and A. J. Sievers, Rev. Mod. Phys. 47, Suppl. 2 (1975).
49. V. Narayanamurti, W. D. Seward, and R. O. Pohl, Phys. Rev. 148 (1966) 481
50. H. J. Jodl and W. B. Holzapfel, Chem. Phy. Lett. 55 (1978) 259.
51. L. A. Rebane, G. S. Zavt, and K. E. Haller, phys. stat. sol. (b) 81 (1977) 57.
52. J.Haldre, L.A. Rebane, A.V. Liapzev, and A.A. Kiselev, phys stat sol (b)70 (1975) 359.
53. A. R. Evans and D. B. Fitchen, Phys. Rev. B2 (1970) 1074.
54. T. Timusk and W. Stuade, Phy. Rev. Lett. 13 (1964) 373.
55. R. Avarmaa and L. Rebane, phys. stat. sol. (b) 35 (1969) 107.
56. G. S. Zavt, phys. stat. sol. (b) 80, 399 (1977).
57. A. J. Sievers and W. E. Moerner, in: Persistent Spectral Hole-Burning: Science and Applications, ed. W. E. Moerner (Springer-Verlag Pub. Co., New York, 1988) Chapter 6.
58. W. Köhler, J. Meiler, and J. Friedrich, Phys. Rev. B 35, 4031 (1987).
59. D. Haarer, in Moerner, ed. , Chapter 3.
60. P.F. Bernath, T. Amano, and M. Wong, J. Mol. Spectry. 98, 20 (1983).
61. W. Rohrbeck, A. Hinz and W. Urban, Mol. Phys. 41, 925 (1980).
62. R. S. Lowe, Mol. Phys. 41, 929 (1980).
63. R. A. Guyer, The Theory of Quantum Crystals, Solid State Physics, Vol. 23, p.413 (edited by F. Seitz, D. Turnbull and H. Ehrenreich) Academic Press, New York (1969).

64. N. R. Werthamer, Am. J. Phys. 37, 963 (1969).

65. L. H. Nosanow, Phys. Rev. 146, 120 (1966); H. W. de Wette, L. H. Nosanow and N. R. Werthamer, Phys. Rev. 162, 824 (1969).

66. E. C. Heltemes and C. A. Swenson, Phys. Rev. 128, 1512 (1962).

67. H. H. Sample and C. A. Swenson, Phys. Rev. 158, 188 (1967).

68. R. C. Pandorf and D. O. Edwards, Phys. Rev. 169, 222 (1968).

69. S. H. Castles and E. D. Adams, Phys. Rev. Lett. 30, 1125 (1973).

70. D. O. Edwards, A. S. Williams, and J. G. Daunt, Phys. Lett. 1, 218 (1962).

71. D. S. Greywall, Phys. Rev.B 15, 2604 (1977).

72. F. W. de Wette and N. R. Werthamer, Phys. Rev. 184, 209 (1968).

73. J. Wilks, The Properties of Liquid and Solid Helium, p. 636, Clarendon Press, Oxford (1967).

74. S. M. Heald, D. R. Baer and R. O. Simmons, Phys. Rev. B 30, 2531 (1984).

75. P. R. Granfors, B. A. Frass and R. O. Simmons, J. of Low Temp. Phys. 67, 353 (1987).

76. R. C. Zeller and R. O. Pohl, Phys. Rev. B 4, 2029 (1971).

77. R. B. Stephens, Phys. Rev. B 8, 2896 (1973).

78. R. O. Pohl, in Amorphous Solids: Low Temperature Properties,ed. W. A. Phillips,Springer Verlag, Berlin, (1981), p. 37.

79. W. A. Phillips, J. Low Temp. Phys.7, 351 (1972).

80. P. W. Anderson, B. I. Halperin and C. M. Varma, Phil. Mag.25, 1 (1972).

81. A. J. Sievers & S. Takeno, Phys. Rev. Lett. 61, 970 (1988).

82. S. Takeno and A. J. Sievers, Sol. St. Commun. 67, 1023 (1988).

83. S. Takeno and A. J. Sievers, Prog. in Theor. Phys. (Suppl. 94) 242, (1988).

84. A. J. Sievers and S. Takeno, Phys. Rev. B 39, Feb. 15 (1989).

85. A. J. Leggett, Ann. Phys. 72, 80 (1972).